



Well-posedness and approximation of reflected McKean-Vlasov SDEs with applications

Downloaded from: <https://research.chalmers.se>, 2025-12-06 18:26 UTC

Citation for the original published paper (version of record):


Hinds, P., Sharma, A., Tretyakov, M. (2025). Well-posedness and approximation of reflected McKean-Vlasov SDEs with applications. *Mathematical Models and Methods in Applied Sciences*, 35(8): 1845-1887. <http://dx.doi.org/10.1142/S0218202525500241>

N.B. When citing this work, cite the original published paper.

Well-posedness and approximation of reflected McKean–Vlasov SDEs with applications

Piers D. Hinds 

*School of Mathematical Sciences,
University of Nottingham, UK
pmaph7@nottingham.ac.uk*

Akash Sharma 

*Department of Mathematical Sciences,
Chalmers University of Technology and the
University of Gothenburg, Sweden
akashs@chalmers.se*

Michael V. Tretyakov 

*School of Mathematical Sciences,
University of Nottingham, UK
Michael.Tretyakov@nottingham.ac.uk*

Received 12 January 2025

Revised 28 March 2025

Accepted 3 April 2025

Published 16 May 2025

Communicated by Nicola Bellomo

In this paper, we establish well-posedness of reflected McKean–Vlasov stochastic differential equations (SDEs) and their particle approximations in smooth non-convex domains. We prove convergence of the interacting particle system to the corresponding mean-field limit with the optimal rate of convergence. We motivate this study with applications to sampling and optimization in constrained domains by considering reflected mean-field Langevin SDEs for sampling and two reflected consensus-based optimization (CBO) models. We utilize reflection coupling to study long-time behavior of reflected mean-field SDEs and also investigate convergence of the reflected CBO models to the

*Corresponding author

This is an Open Access article published by World Scientific Publishing Company. It is distributed under the terms of the Creative Commons Attribution 4.0 (CC BY) License, which permits use, distribution and reproduction in any medium, provided the original work is properly cited.

global minimum of a constrained optimization problem. We numerically test reflected CBO models on benchmark constrained optimization problems and an inverse problem.

Keywords: Interacting particle system, constrained optimization, constrained sampling, mean-field Langevin dynamics, consensus-based optimization, reflected mean-field diffusion, reflected stochastic differential equations, propagation of chaos.

AMS Subject Classification 2020: 60H10 90C26 65C30 65C35 60J76

1. Introduction

Reflected stochastic differential equations (SDEs) are used to model processes confined to a domain with boundary, where the solution is reflected along a certain direction when it hits the boundary. At the same time, McKean–Vlasov SDEs have coefficients with nonlinear dependencies on the law of the solution. This paper is devoted to the study of reflected McKean–Vlasov SDEs which can model systems with constraints and mean-field interactions. We illustrate practical relevance of reflected mean-field SDEs via problems in sampling and optimization with constraints.

Sampling and optimization problems are ubiquitous in the applied sciences and have found resurgence due to advancements in machine learning. The relation between optimization and sampling is quite established. While convex optimization (as well as log-concave sampling) is well-studied,⁵³ the task of non-convex global optimization (as well as non-log-concave sampling) poses additional challenges.³⁴ In the Bayesian setting, many of the optimization problems can be posed as sampling problems. On the other hand, many sampling techniques can be viewed as optimization in infinite dimensional setting through the variational perspective. With regard to global optimization, *metaheuristic methods* are a popular class of methods which have been used to numerically solve global optimization problems. Such methods consist of a high-level algorithmic framework to coordinate low-level heuristics in order to efficiently explore and exploit the solution space. Examples include particle swarm optimization³⁹ and differential evolution⁶² among others. While there is typically limited theoretical foundation for such models, these methods have been found to be effective in practice.⁶⁸ We are mainly interested in optimization and sampling techniques based on interacting particle systems driven by reflected SDEs.

Interacting particle system-based models have resulted in better understanding of many natural and social phenomena.^{5, 6, 14, 32} Therefore, it is not surprising that interacting particle-based methods for optimization and sampling have also gained traction (see Refs. 40, 13, 47, 28, 29, 57 and 38) due to their enhanced capability to explore a non-convex energy landscape. These systems are driven by SDEs and hence the tools from stochastic calculus, especially mean-field theory⁶⁴ and stochastic numerics⁵² are available to establish their convergence.

Let us discuss the contributions of this paper along with the comparison with existing literature. We will further discuss the literature at appropriate places later in the paper. Here, we give a high-level overview. In the paper, we first estab-

lish existence and uniqueness of reflected McKean–Vlasov SDEs and their particle approximations in a non-convex domain setting (Sec. 3). The well-posedness was shown in a convex domain setting in Ref. 1 and in a non-convex setting, but allowing only first-order interaction, in Ref. 63. In Ref. 69 well-posedness was also considered in a non-convex domain setting but for McKean–Vlasov SDEs with singular drift and extra conditions on the diffusion coefficient. Our next result is convergence of the interacting particle system towards its mean-field limit with the optimal rate of convergence (Sec. 4). The assumptions that we impose for well-posedness and particle convergence are general enough that many models which have been studied in \mathbb{R}^d (see e.g. Refs. 13, 28, 15 and 22) can be reformulated in the framework of reflected McKean–Vlasov SDEs to handle constraints to which results of this paper can be applied. We provide three illustrations for application of reflected McKean–Vlasov SDEs to sampling and optimization. The first one is reflected mean-field Langevin dynamics (Sec. 2.1) for which we employ reflection coupling to study its long-time behavior and obtain non-asymptotic bounds (Sec. 5.1). In the convex domain setting, this study was conducted in Ref. 70. The second class of models we consider is consensus-based optimization (CBO) models (Sec. 2.2) for which we establish convergence to the global minimum (Sec. 5.2). We add a repelling force in the CBO model to enhance exploration (Sec. 2.2.2) and observe its benefits in numerical testing on the Rosenbrock function (Sec. 6.5). We test two discretization schemes for reflected SDEs, namely the penalty and projection schemes, to implement the CBO models for a few benchmark constrained optimization problems including an inverse problem (Sec. 6).

A natural question that arises is why one would formulate optimization and sampling problems with constraints in the setting of reflected SDEs. We first mention other strategies which have been proposed and employed to handle constraints in the literature on interacting particle systems driven by SDEs for the purpose of optimization and sampling. In Ref. 10, a CBO model is considered where a penalty function is added to the objective function f , which penalizes the objective when points are outside the feasible set \bar{G} (f is defined on \mathbb{R}^d). For a penalization multiplier $\epsilon > 0$, the following unconstrained problem is considered:

$$\min_{x \in \mathbb{R}^d} P(x; \epsilon), \quad (1.1)$$

where $P(x; \epsilon) = f(x) + \epsilon r(x)$ with $r(x) > 0$ if the feasible set \bar{G} is violated else it is zero. An Euler scheme is applied to simulate the corresponding particle system. Convergence of the algorithm to the optimal solution is shown, both when the exact penalty parameter ϵ is known, and also when it is iteratively updated. In Ref. 18, like Ref. 10, the authors also use a penalized objective function presenting several numerical experiments. In Ref. 3, a projection technique is considered for discrete time CBO model driven by common noise. It is observed in numerical tests on benchmark functions that common noise may result in less exploration producing a sub-standard performance (see Ref. 38). In the case of ensemble Kalman inversion, which is again an interacting particle-based optimization method for inverse

problems (see e.g. Ref. 36), in Ref. 19 box constraints are handled using projection scheme and in Ref. 33 a log-barrier penalty is added to deal with inequality constraints defining the convex feasible region.

We now illustrate with a simple example to highlight why reflected SDEs (i.e. Skorokhod's dynamics) are the natural candidates to handle constraints in models arising not only in biological and physical sciences but also in models underlying sampling and optimization techniques. Suppose, we are interested in minimizing a continuously differentiable Lipschitz function $f : \bar{G} \rightarrow \mathbb{R}$ where $G \subset \mathbb{R}^d$ is a convex domain with boundary ∂G , and $x_{\min} = \arg \min_{x \in \bar{G}} f(x)$ is the unique global minimum. In the continuous-time setting, we can employ the following gradient dynamics posed as Skorokhod's problem:

$$dX(t) = -\nabla f(X(t))dt + dK(t), \quad X(0) \in G,$$

where $K(t)$ is a finite variation process which restricts $X(t)$ within \bar{G} . We call the pair $(X(t), K(t))$ the solution of the Skorokhod problem, whose existence and uniqueness in the convex domain setting is proved by Tanaka.⁶⁵ The process $K(t)$ can be written as

$$K(t) = \int_0^t I_{\partial G}(X(s)) \nu(X(s)) d|K|(s),$$

where $|K|(t)$ is the total variation of $K(t)$, $\nu(x)$ is an inward normal at $x \in \partial G$, and $I_{\partial G}(x)$ is indicator function which takes value 1 if $x \in \partial G$ else 0. Using the chain rule, we get

$$\begin{aligned} d|X(t) - x_{\min}|^2 &= -2((X(t) - x_{\min}) \cdot \nabla f(X(t)))dt \\ &\quad + 2I_{\partial G}(X(t))((X(t) - x_{\min}) \cdot \nu(X(t)))d|K|(t). \end{aligned}$$

Note that ν is the inward normal of the convex domain G , and if we take f to be strongly convex, then we have for some $\kappa > 0$

$$\begin{aligned} ((X(t) - x_{\min}) \cdot \nabla f(X(t))) &\geq \kappa |X(t) - x_{\min}|^2 \quad \text{and} \\ I_{\partial G}(X(t))((X(t) - x_{\min}) \cdot \nu(X(t))) &\leq 0. \end{aligned}$$

This results in $d|X(t) - x_{\min}|^2 \leq -2\kappa |X(t) - x_{\min}|^2 dt$ and hence $|X(t) - x_{\min}|^2 \leq |X(0) - x_{\min}|^2 e^{-2\kappa t}$. It means $X(t) \rightarrow x_{\min}$ as $t \rightarrow \infty$.

In a similar manner, if f and G are such that

$$(\nabla f(x) \cdot \nu(x)) \leq 0, \quad x \in \partial G, \tag{1.2}$$

then via chain rule we have $d(f(X(t)) - f(x_{\min})) \leq -|\nabla f(X(t))|^2 dt$. If, in addition, we assume that Polyak's inequality holds for f with constant $\eta > 0$, then $d(f(X(t)) - f(x_{\min})) \leq -\eta(f(X(t)) - f(x_{\min}))dt$ and hence $(f(X(t)) - f(x_{\min})) \leq (f(X(0)) - f(x_{\min}))e^{-\eta t}$.

Although above we have taken the example of deterministic convex constrained optimization, it conveys the strategy of using reflected dynamics. In contrast to the approaches of penalizing the objective function (see e.g. Refs. 18, 10 and 3), here

we do not need to modify $f(x)$, noting that modifying $f(x)$ so that it preserves the global optimum within/near the constraint set \bar{G} is not a trivial task, especially in high dimensions. Moreover, introducing artificial barriers in the objective function typically leads to SDEs with their coefficients taking very large values outside the domain \bar{G} (effectively, making the SDEs very stiff) which in turn requires use of numerical methods approximating these stiff SDEs with small time steps or of complex nature. This problem does not arise within the reflected SDEs setting considered in this work.

Further, as it has been seen from the above example, we can split our analysis into two steps. In the first step, we establish convergence of continuous-time dynamics to the desired quantity, which can be the global minimum in an optimization scenario or a functional of the desired measure in the case of sampling. The next step is to approximate these continuous-time reflected dynamics, for which a plethora of numerical discretization schemes are available to us. Each of these schemes can be considered as an optimization or sampling technique. For weak-sense approximation (i.e. approximating expectation of function of dynamics with sufficiently large class of functions), we have Lepingle's procedure in the half space setting,⁴⁴ Milstein's change of coordinates scheme,⁵¹ the half-space Euler scheme,³⁰ symmetrized-reflected scheme,^{11, 41} and specularly reflected scheme.⁴² All these numerical schemes are analyzed in a non-convex setting except Ref. 44. For mean-square (strong) approximation, we have the projection scheme^{54, 61} and the penalty scheme.⁶¹ We mention that projection and penalty schemes have only been analyzed in the convex bounded domain setting, and even then with suboptimal convergence rate (except when the domain is a convex polytope). We note that study of numerical approximation of reflected SDEs is not the aim of this paper, rather we are interested in well-posedness of mean-field SDEs, their particle approximation, and their large time behavior as well as in their applications.

In Sec. 2, we introduce the set-up of reflected nonlinear (in the sense of McKean) SDEs and describe applications to sampling and optimization. We establish well-posedness in Sec. 3 and prove propagation of chaos in the strong sense in Sec. 4. We devote Sec. 5 to large time investigation of reflected mean-field SDE with additive noise and CBO models. The last section (Sec. 6) contains several numerical experiments to validate the performance of CBO models with convex as well as non-convex constraints.

Before moving to the following section, we mention the notation used throughout the paper. We denote $(a \cdot b)$ as scalar product between two vectors $a, b \in \mathbb{R}^d$. At certain places, we have also used the notation $a^\top b$ to avoid unnecessary confusion due to many brackets. If A is a square matrix, $\text{tr}(A)$ represents its trace. We denote by ∇f and $\nabla^2 f$ the gradient and Hessian, respectively, of a scalar-valued function $f : \mathbb{R}^d \rightarrow \mathbb{R}$. We use the notation $|\cdot|$ for Frobenius norm of a $d \times n$ matrix. For $n = 1$, it reduces to Euclidean norm. We denote by $\text{Diag}(a)$, a diagonal matrix whose diagonal is given by $a \in \mathbb{R}^d$. We use C as a generic positive constant whose value may change from line to line.

2. Reflected McKean–Vlasov SDEs

In this section, we first introduce reflected mean-field SDEs and their particle approximation. Then we illustrate their applications in solving constrained optimization and sampling problems.

Let $\mathcal{P}(\bar{G})$ be the space of probability measures on \bar{G} and $b : \mathbb{R}_+ \times \bar{G} \times \mathcal{P}(\bar{G}) \rightarrow \mathbb{R}^d$ and $\sigma : \mathbb{R}_+ \times \bar{G} \times \mathcal{P}(\bar{G}) \rightarrow \mathbb{R}^{d \times d}$. We will impose conditions on these coefficients later. By $\nu(x)$, we denote the unit inward normal at point x belonging to boundary ∂G . Let $(\Omega, \mathcal{F}, \mathbb{P})$ be a complete, sufficiently rich probability space and \mathcal{F}_t , $0 \leq t \leq T$, be a filtration satisfying the usual hypothesis. Let $(W(t), \mathcal{F}_t)$ and $(\mathbf{W}(\mathbf{t}), \mathcal{F}_t)$ be standard d -dimensional and Nd -dimensional Wiener processes, respectively, with $\mathbf{W}(\mathbf{t}) = (W^1(t), \dots, W^N(t))^T$, where $W^i(t)$ are independent standard d -dimensional Wiener processes. We will also use the notation: \mathcal{F}_t^W is the natural filtration for the Wiener process $W(t)$ and $\mathcal{F}_t^{\mathbf{W}}$ is the natural filtration for the Wiener process $\mathbf{W}(\mathbf{t})$.

Consider a nonlinear (in the sense of McKean) Markov process evolving on \bar{G} driven by the SDEs

$$\begin{aligned} X(t) = X(0) + \int_0^t b(s, X(s), \mathcal{L}_{X(s)}) ds + \int_0^t \sigma(s, X(s), \mathcal{L}_{X(s)}) dW(s) \\ + \int_0^t \nu(X(s)) I_{\partial G}(X(s)) dL(s), \quad X(0) \in \bar{G}, \end{aligned} \quad (2.1)$$

where $\mathcal{L}_{X(s)}$ is the time marginal law of $X(s)$, and $L(s)$ is a scalar non-decreasing process which increases only when $X(s) \in \partial G$ (see the precise definition in e.g. Refs. 46, 37 and 26): $L(t) = \int_0^t I_{\partial G}(X(s)) dL(s)$ a.s. We also note (see Ref. 46) that the integral form of the local time term of (2.1), $K(t) = \int_0^t \nu(X(s)) I_{\partial G}(X(s)) dL(s)$, is a d -dimensional bounded variation process.

The first step towards implementation of models based on (2.1) is their particle approximation. Let δ_x be the Dirac measure defined as $\delta_x(A) = I_A(x)$ with A being a measurable set and, for a collection of random variables written in the tuple form as $\mathbf{Z} = (Z^1, \dots, Z^N)^\top$, define the empirical measure

$$\hat{\mu}_{\mathbf{Z}} = \frac{1}{N} \sum_{i=1}^N \delta_{Z^i}. \quad (2.2)$$

The system of N interacting particles takes the form

$$\begin{aligned} X^{i,N}(t) = X^{i,N}(0) + \int_0^t b(s, X^{i,N}(s), \hat{\mu}_{\mathbf{X}^N(s)}) ds \\ + \int_0^t \sigma(s, X^{i,N}(s), \hat{\mu}_{\mathbf{X}^N(s)}) dW^i(s) \\ + \int_0^t \nu(X^{i,N}(s)) I_{\partial G}(X^{i,N}(s)) dL^{i,N}(s), \quad X^{i,N}(0) \in \bar{G}, \end{aligned} \quad (2.3)$$

where $\mathbf{X}^N(t) = (X^{1,N}(t), \dots, X^{N,N}(t))^\top$ and $L^{i,N}(t)$ is the local time of the i th particle on the boundary ∂G . In Sec. 3, we establish well-posedness of (2.1) and

(2.3) under some general assumptions on the coefficients and the domain, and in Sec. 4, we prove convergence of the particle system to its mean-field limit (2.1). In Sec. 5.1, we study large-time behavior of (2.1) with $\sigma \equiv I$ via reflection coupling.

Different choices of b and σ in (2.1) can lead to particular models for solving constrained optimization and sampling problems. In Sec. 2.1, we present reflected mean-field Langevin SDEs which can be used for sampling from nonlinear measure with compact support. In Secs. 2.2.1 and 2.2.2, based on (2.1), we present two optimization methods of the CBO-type which we later analyze. The CBO methods are derivative-free. Although we present mean-field Langevin and CBO-type models as examples of reflected mean-field SDEs, we highlight that one can also write reflected versions of other interacting particle-based sampling and optimization models for which our results on well-posedness from Sec. 3 and convergence of the particle approximation with the optimal rate from Sec. 4 hold by verifying the assumptions without difficulty. Ensemble Kalman–Langevin sampler is proposed for sampling in Ref. 28. Its dynamics orchestrate the interaction among particles via ensemble covariance matrix and also utilize gradient information, making it a gradient-based method. The model can be used for constrained sampling by formulating it within the reflected SDEs setting and can also be turned into a constrained optimization model by exploiting the fact that the measure concentrates on the global minimum for lower temperature. Hence, in this case, this model can be written in the form (2.3). The same can be said for swarm gradient dynamics with measure-dependent annealing studied in Ref. 22 and swarm dynamics of Ref. 9 which can be put in the framework of reflected SDEs for constrained optimization. As already mentioned, since we prove our results of well-posedness of reflected McKean–Vlasov SDEs and interacting particle system in Sec. 3 and propagation of chaos result in Sec. 4 for general SDEs, these results are applicable to all the above-mentioned additional models without any difficulty. These existence and convergence results will also hold true, with minor modifications, for reflected versions of mean-field ODE-based models like the Stein variational gradient descent⁴⁷ and ensemble Kalman inversion (noise-free setting)^{57, 58} for sampling and optimization, respectively.

2.1. Reflected mean-field Langevin dynamics

Consider the following mean-field Langevin dynamics with reflection:

$$\begin{aligned} dX(t) = & -\nabla U(X(t))dt - \int_{\bar{G}} \nabla V(X(t) - y) \mathcal{L}_{X(t)}(dy) + \sigma dW(t) \\ & + \nu(X(t))dL(t), \end{aligned} \quad (2.4)$$

where $U : \bar{G} \rightarrow \mathbb{R}$ is an external potential, $V : \bar{G} \rightarrow \mathbb{R}$ is an interaction potential, and $\sigma > 0$. The primary motivation for this model comes from statistical physics. In \mathbb{R}^d its well-posedness and convergence to equilibrium were studied in Refs. 48 and 17. The propagation of chaos with singular interaction potential (and no external potential) has been considered in Ref. 24 in a convex bounded domain setting. This

object has recently gathered more interest due to its link to the mean-field point of view on neural networks.^{35, 49, 60} Empirical investigation in Ref. 43 suggests that constraint training of neural networks can avoid over-fitting and provide stability. In the mean-field point of view, the problem of training a two-layer wide network with constraints can be posed as the mean-field reflected dynamics (2.4).

Let us denote by $(V * \mu)(x)$ the convolution $\int_{\bar{G}} V(x - y)\mu(dy)$. The nonlinear measure given by

$$\tilde{\mu} \propto \exp\left(-\frac{2}{\sigma^2}(U + V * \tilde{\mu})\right) \quad (2.5)$$

is invariant for the nonlinear Markov processes evolving according to the mean-field Langevin dynamics (2.4) on \bar{G} . This can be confirmed by checking that the density ρ of the measure $\tilde{\mu}$ satisfies the (nonlinear) stationary Fokker–Planck equation:

$$-\nabla \cdot (\rho(x)b(x, \rho)) + \frac{\sigma^2}{2}\Delta\rho(x) = 0, \quad x \in G, \quad (2.6)$$

with boundary condition:

$$\frac{\sigma^2}{2}(\nabla\rho(x) \cdot \nu(x)) - (b(x, \rho) \cdot \nu(x))\rho(x) = 0, \quad x \in \partial G, \quad (2.7)$$

where $b(x, \rho) = -\nabla U(x) - \int_{\bar{G}} \nabla V(x - y)\rho(y)dy$. Long-time simulation of the nonlinear SDEs (2.4) can produce samples from the implicitly defined measure (2.5) supported on \bar{G} . If the coefficients satisfy Assumption 4.1 (which does not require convex U or V) then it ensures the optimal rate of convergence for particle approximation to mean-field limit (see Theorem 4.1). The result of Sec. 5.1 regarding weak convergence towards equilibrium holds for (2.4) also allowing for non-convex potentials U and V .

2.2. Reflected consensus-based models

In this section, we consider consensus-based models in the form of reflected SDEs which can be used for solving the constrained optimization problem:

$$\min_{x \in \bar{G}} f(x), \quad (2.8)$$

where $f : \bar{G} \rightarrow [0, \infty)$ is an objective function (which can be non-convex) and $G \subset \mathbb{R}^d$ is a bounded domain with a sufficiently smooth boundary ∂G (see Assumption 3.1). Since \bar{G} is compact, f obtains its infimum and supremum over \bar{G} .

Assumption 2.1. (Objective function) (i) The objective function satisfies

$$f_{\min} := \inf_{x \in \bar{G}} f(x) > 0, \quad (2.9)$$

and the minimizer of f , denoted as x_{\min} is unique, i.e. there is only $x_{\min} \in \bar{G}$ such that $f(x_{\min}) = f_{\min}$.

(ii) There exists $L_f > 0$ such that

$$|f(x) - f(y)| \leq L_f |x - y|, \quad (2.10)$$

for all $x, y \in \bar{G}$.

If f is continuously differentiable then (2.10) is automatically satisfied. We denote the supremum of f as

$$f_{\max} = \sup_{x \in \bar{G}} f(x). \quad (2.11)$$

2.2.1. Reflected consensus-based optimization

In Ref. 56, the metaheuristic method of CBO was introduced. In this model, the energy landscape of the objective function is explored by N interacting particles. Each particle broadcasts its current location to the other particles via an average location, which is weighted according to the energy landscape: particles where the objective function is small are given higher weights than those where the objective function is large. The position of each particle updates continuously so that each particle drifts towards this weighted average, whilst also exploring its current neighborhood through random perturbations. These dynamics allow for the continuous-time formulation of the CBO model via SDEs. The mathematical framework for CBO has been developed in Refs. 13, 16, 31 and 38. A survey on the topic is available in Ref. 66.

Let us present the reflected version of mean-field consensus-based dynamics (see also Ref. 4):

$$\begin{aligned} dX(t) = & -\beta(X(t) - \bar{X}(t))dt + \sigma \text{Diag}(X(t) - \bar{X}(t))dW(t) \\ & + \nu(X(t))I_{\partial G}(X(t))dL(t), \end{aligned} \quad (2.12)$$

where the weighted mean $\bar{X}(t)$ (depending on the objective f and some $\alpha > 0$) is

$$\bar{X}(t) := \bar{X}(\mathcal{L}_{X(t)}) := \frac{\int_{\bar{G}} x e^{-\alpha f(x)} \mathcal{L}_{X(t)}(dx)}{\int_{\bar{G}} e^{-\alpha f(x)} \mathcal{L}_{X(t)}(dx)}, \quad (2.13)$$

$\beta > 0$ and $\sigma > 0$ are constant (see a discussion in Ref. 38 on potential benefits of choosing them dependent on time). The relationship between β and σ required for convergence of $X(t)$ to the global minimum x_{\min} will be established within convergence analysis in Sec. 5.2.

The particle approximation of (2.12) is given by

$$\begin{aligned} dX^{i,N}(t) = & -\beta(X^{i,N}(t) - \bar{X}^N(t))dt + \sigma \text{Diag}(X^{i,N}(t) - \bar{X}^N(t))dW^i(t) \\ & + \nu(X^{i,N}(t))I_{\partial G}(X^{i,N}(t))dL^{i,N}(t), \quad X^{i,N}(0) = X_0^{i,N}, \end{aligned} \quad (2.14)$$

where the weighted mean $\bar{X}^N(t)$ is

$$\bar{X}^N(t) := \bar{X}^{N,f,\alpha}(t) := \frac{\sum_{i=1}^N X^{i,N}(t) e^{-\alpha f(X^{i,N}(t))}}{\sum_{i=1}^N e^{-\alpha f(X^{i,N}(t))}}, \quad (2.15)$$

which we will refer to as the particles' consensus. In corresponding particles system (2.14), the particles interact with each other via (2.15) and try to realize a uniform consensus.

Constrained CBO has been considered in Refs. 10, 3 and 18. The distinction of our work lies in the fact that we encode the constraints into the continuous-time model with the use of reflected SDEs. While completing this work, we became aware of Ref. 4, where the model (2.12) is also considered. In the convex domain setting, well-posedness, convergence of particle approximation and convergence of CBO model to its global minimum are shown in Ref. 4 using Tanaka's trick (note that for more general mean-field SDE in convex domains well-posedness and propagation of chaos were earlier proved in Ref. 1). Here, we consider CBO and its new modified version with repelling forces in the following subsection as examples and prove well-posedness and convergence of particle system in non-convex domains satisfying the uniform exterior sphere condition. For showing convergence to global minimum, we switch to a convex setting and employ techniques introduced in Ref. 16. We discuss in detail the reasoning behind moving to the convex setting in Sec. 5.2 and provide useful insight for further development of CBO models. In addition to the projection numerical method for approximating reflected SDEs (also used in Ref. 4), we also investigate performance of the penalty scheme for constrained optimization.

2.2.2. *Reflected consensus-based optimization with attracting and repelling forces*

In the reflected CBO model (2.12), the particles are attracted towards their weighted mean portraying exploiting behavior based on already searched space, and the exploration is achieved thanks to noise induced by independent Brownian motions driving each particle. In Ref. 38, the exploration is enhanced by adding compound Poisson processes. Another way to facilitate exploration is by incorporating repelling forces among particles with a decaying parameter. The model embodying both attractive and repelling behavior takes the form

$$\begin{aligned} dX(t) = & -\beta(X(t) - \bar{X}(t))dt \\ & + \lambda(t) \int_G (X(t) - y) \exp\left(-\frac{1}{2}|X(t) - y|^2\right) \mathcal{L}_{X(t)}(dy)dt \\ & + \sigma \text{Diag}(X(t) - \bar{X}(t))dW(t) + \nu(X(t))I_{\partial G}(X(t))dL(t), \end{aligned} \quad (2.16)$$

and its particle approximation is given by

$$\begin{aligned} dX^{i,N}(t) = & -\beta(X^{i,N}(t) - \bar{X}^N(t))dt \\ & + \frac{\lambda(t)}{N} \sum_{j=1}^N (X^{i,N}(t) - X^{j,N}(t)) \exp\left(-\frac{1}{2}|X^{i,N}(t) - X^{j,N}(t)|^2\right)dt \\ & + \sigma \text{Diag}((X^{i,N}(t) - \bar{X}^N(t)))dW^i(t) + \nu(X^{i,N}(t))I_{\partial G}(X^{i,N}(t))dL^{i,N}(t). \end{aligned} \quad (2.17)$$

Here, $\beta > 0$ and $\sigma > 0$ are constant, and $\lambda(t) \geq 0$ is a decreasing function of t and preferably should have exponential decay in later steps of the method. The repelling

force between any two particles decays as the distance between the two particles increases in order to ensure there is no explosion in the dynamics. When particles are close to each other they experience greater repelling to avoid collapse of the ensemble at a local minimum. The relation among β , σ and λ will be discussed in Sec. 5.2.

3. Well-Posedness Results

In this section, we aim to show: (i) well-posedness of the mean-field SDEs (2.1) (existence and uniqueness; Sec. 3.1) and (ii) well-posedness of the particle system (2.3) (existence and uniqueness; Sec. 3.2). We also verify (Sec. 3.3) that the assumptions imposed on the coefficients of (2.1) and on the domain G under which these well-posedness results hold are satisfied for the two CBO models from Secs. 2.2.1 and 2.2.2.

3.1. Well-posedness of reflected McKean–Vlasov SDEs

If G were a convex domain, then it is easier to deal with the local time term in (2.1) using Tanaka’s trick⁶⁵ which is exploited in the McKean–Vlasov setting in Ref. 1. Here, we do not assume that G is convex, but instead assume that G is bounded and rely on the boundary ∂G satisfying the uniform exterior sphere condition. Sznitman⁶³ considered this case of non-convex G but only for a first-order interaction. Note that the optimization and sampling models discussed in Sec. 2 do not fall into this category, and hence we study the general mean-field SDEs (2.1).

The standard way to prove existence and uniqueness is to appeal to a fixed point argument. To do this, one shows that the map from an arbitrary measure to the measure of the solution of the mean-field SDEs constructed from the arbitrary measure is a contraction. In our setting, this standard fixed-point argument can be used. The existence and uniqueness of a fixed point corresponds to the existence and uniqueness of a solution to the reflected mean-field SDEs (2.1).

For a measurable space $(S, \mathcal{B}(S))$, denote by $\mathcal{P}(S)$ the space of probability measures on S . We use the notation: $\mathcal{C} = C(\mathbb{R}_+, \bar{G})$ equipped with the Borel σ -algebra generated by the uniform norm topology and $\mathcal{M} = \mathcal{P}(\mathcal{C})$. For a measure $\mu \in \mathcal{M}$, we denote by μ_t its projection onto $\mathcal{P}(\bar{G})$ at time t , i.e. its marginal:

$$\mu_t(A) = \int_{\mathcal{C}} I_A(w_t) d\mu(w), \quad A \in \mathcal{B}(\bar{G}). \quad (3.1)$$

For two measures $\mu^1, \mu^2 \in \mathcal{P}(\bar{G})$, the Wasserstein p -metric is defined as

$$\mathcal{W}_p(\mu^1, \mu^2) := \inf_{\gamma \in \Gamma(\mu^1, \mu^2)} \left[\int_{\bar{G} \times \bar{G}} |x - y|^p d\gamma(x, y) \right]^{\frac{1}{p}}, \quad (3.2)$$

where $\Gamma(\mu^1, \mu^2)$ denotes the set of couplings between μ^1 and μ^2 .

Assumption 3.1. The domain $G \subset \mathbb{R}^d$ is bounded and its boundary ∂G is C^3 .

The smoothness of the boundary assumed here is required so that the distance function to the boundary of G , $d(\cdot, \partial G)$, defined on a neighborhood of ∂G is C^2 (see e.g. Lemma 1 in Sec. 3 of Ref. 59). We make use of this in Theorem 3.1.

Assumption 3.2. (Uniformly Lipschitz in space and measure) There exists $L > 0$ such that for all $t \geq 0$

$$|b(t, x, \mu^1) - b(t, y, \mu^2)| + |\sigma(t, x, \mu^1) - \sigma(t, y, \mu^2)| \leq L(|x - y| + \mathcal{W}_4(\mu^1, \mu^2)), \quad \forall x, y \in \bar{G}, \quad \forall \mu^1, \mu^2 \in \mathcal{P}(\bar{G}). \quad (3.3)$$

Also, the coefficients $b(t, x, \mu)$ and $\sigma(t, x, \mu)$ are continuous in t .

Since ∂G is sufficiently smooth, it satisfies the uniform exterior sphere condition. That is, there exists $R_0 > 0$ such that $\forall x \in \partial G$,

$$\bar{B}(x - R_0\nu(x), R_0) \cap \partial G = \{x\},$$

where $\bar{B}(x, R_0)$ denotes the closed ball of radius R_0 centered at x and $\nu(x)$ is the inward normal vector field at $x \in \partial G$. The constant r is called the uniform exterior sphere constant of G . This is equivalent to the following condition:

$$\exists c \geq 0, \quad \forall x \in \partial G, \quad \forall y \in \bar{G}, \quad c|x - y|^2 \geq (x - y)^\top \nu(x), \quad (3.4)$$

see for example Refs. 46 and 55. The constant c is related to the uniform exterior sphere constant by $c = \frac{1}{2R_0}$.

Theorem 3.1. *Let Assumptions 3.1 and 3.2 hold. There exists a unique pair of continuous \mathcal{F}_t^W -adapted processes $(X(t), L(t))$ such that (i) $X(t) \in \bar{G}$ for all $t \geq 0$; (ii) $L(t)$ is non-decreasing with $L(0) = 0$ and for all $t \geq 0$,*

$$L(t) = \int_0^t I_{\partial G}(X(s)) dL(s); \quad (3.5)$$

and (iii) for all $t \geq 0$,

$$X(t) = X(0) + \int_0^t b(s, X(s), \mathcal{L}_{X(s)}) ds + \int_0^t \sigma(s, X(s), \mathcal{L}_{X(s)}) dW(s) + \int_0^t \nu(X(s)) dL(s). \quad (3.6)$$

Such a theorem is proved in Ref. 63 in the case of first-order interaction rather than (2.1). Our proof of Theorem 3.1 borrows certain arguments and notation from Ref. 63 which also draws techniques from Ref. 46 to deal with the local time term.

For brevity, we denote $X_s := X(s)$, $W_s := W(s)$, and $L_s := L(s)$. Consider the map $\Phi : \mathcal{M} \rightarrow \mathcal{M}$ defined by $\Phi(\mu) = \mathcal{L}_{Y^\mu}$, where $\mu \in \mathcal{M}$ and \mathcal{L}_{Y^μ} is the law of $\{Y_t^\mu\}_{t \geq 0}$ which is defined as

$$Y_t^\mu = X_0 + \int_0^t b(s, Y_s^\mu, \mu_s) ds + \int_0^t \sigma(s, Y_s^\mu, \mu_s) dW_s + \int_0^t \nu(Y_s^\mu) I_{\partial G}(Y_s^\mu) dL_s. \quad (3.7)$$

The process Y is decoupled from its own measure and, as such, is just an ordinary reflected SDE. The existence and uniqueness of a solution to (3.7) is proved in Ref. 46 when the coefficients b and σ are defined on the whole space \mathbb{R}^d . We note that we can extend our coefficients smoothly to the whole space, and the choice of extension does not affect the solution Y^μ . Hence, the map Φ is well-defined. From the definition of Φ , if Φ has a unique fixed point, then the processes associated with this fixed point are the unique solution to (2.1). Our objective is to show that there exists a unique fixed point by demonstrating that, for some j , the j -fold composition, Φ^j , is a contraction.

Let us fix an arbitrary $T > 0$ and consider the space $\mathcal{C}_T = C([0, T], \bar{G})$ and $\mathcal{M}_T := \mathcal{P}(\mathcal{C}_T)$ equipped with the metric

$$D_T(\mu^1, \mu^2) = \inf_{\gamma \in \Gamma(\mu^1, \mu^2)} \left[\int_{\mathcal{C}_T \times \mathcal{C}_T} \left(\sup_{s \leq T} |X(s) - Y(s)| \right)^4 d\gamma(X, Y) \right]^{\frac{1}{4}}.$$

Note that D_T is the Wasserstein 4-distance with respect to the norm $\sup_{s \leq T} |X(s)|$, $X \in \mathcal{C}_T$. Completeness of the space (\mathcal{M}_T, D_T) follows from separability and completeness of $(\mathcal{C}_T, \sup_{s \leq T} |X(s) - Y(s)|)$ (see Refs. 7 and 8).

To prove Theorem 3.1, we need the following lemma.

Lemma 3.1. *Under Assumptions 3.1 and 3.2, there exists $K_T > 0$ such that for all $\mu_1, \mu_2 \in \mathcal{M}$,*

$$D_T^4(\Phi(\mu^1), \Phi(\mu^2)) \leq K_T \int_0^T D_u^4(\mu^1, \mu^2) du. \quad (3.8)$$

Proof. Let $\mu^1, \mu^2 \in \mathcal{M}$ and define the processes $Y_t^1 := Y_t^{\mu^1}$, $Y_t^2 := Y_t^{\mu^2}$ via (3.7). Denote by $d(\cdot, \partial G)$ the distance to the boundary of G , defined on some neighborhood of ∂G within G and let the function $g(\cdot)$ be a smooth, bounded extension of it to the whole space. Then Ito's formula gives

$$\begin{aligned} g(Y_t^i) &= g(X_0) + \int_0^t \nabla g^\top(Y_s^i) b(s, Y_s^i, \mu_s^i) + \frac{1}{2} \text{tr}[\sigma(s, Y_s^i, \mu_s^i)^\top \nabla^2 g(Y_s^i) \sigma(s, Y_s^i, \mu_s^i)] ds \\ &\quad + \int_0^t \nabla g^\top(Y_s^i) \sigma(s, Y_s^i, \mu_s^i) dW_s + \int_0^t \nabla g^\top(Y_s^i) \nu(Y_s^i) dL_s \end{aligned} \quad (3.9)$$

for $i = 1, 2$, where ∇^2 denotes the Hessian. Noting that $\nabla g = \nu$ on ∂G , we have

$$\int_0^t \nabla g^\top(Y_s^i) \nu(Y_s^i) dL_s = L_t. \quad (3.10)$$

In the interest of brevity, we then write (3.9) as

$$g_t^i = g_0 + \int_0^t \left(\nabla g_s^{i\top} b_s^i + \frac{1}{2} \text{tr}[\sigma_s^{i\top} \nabla^2 g_s^i \sigma_s^i] \right) ds + \int_0^t \nabla g_s^{i\top} \sigma_s^i dW_s + L_t^i, \quad i = 1, 2. \quad (3.11)$$

Let $c > 0$ be the uniform exterior sphere constant from (3.4). By Ito's formula, we have

$$\begin{aligned} \exp\{-2c(g_t^1 + g_t^2)\} &= \exp\{-4cg_0\} + \int_0^t \exp\{-2c(g_s^1 + g_s^2)\}(-2c\tilde{b}_s + 2c^2\tilde{\sigma}_s\tilde{\sigma}_s^\top)ds \\ &\quad - \int_0^t 2c \exp\{-2c(g_s^1 + g_s^2)\}\tilde{\sigma}dW_s \\ &\quad - \int_0^t 2c \exp\{-2c(g_s^1 + g_s^2)\}[dL_s^1 + dL_s^2], \end{aligned} \quad (3.12)$$

where

$$\begin{aligned} \tilde{b}_s &= (\nabla g_s^1)^\top b_s^1 + (\nabla g_s^2)^\top b_s^2 + \frac{1}{2}\text{tr}[(\sigma_s^1)^\top \nabla^2 g_s^1 \sigma_s^1 + (\sigma_s^2)^\top \nabla^2 g_s^2 \sigma_s^2], \\ \tilde{\sigma}_s &= (\nabla g_s^1)^\top \sigma_s^1 + (\nabla g_s^2)^\top \sigma_s^2. \end{aligned} \quad (3.13)$$

Also,

$$\begin{aligned} |Y_t^1 - Y_t^2|^2 &= \int_0^t (2(Y_s^1 - Y_s^2)^\top (b_s^1 - b_s^2) + \text{tr}[(\sigma_s^1 - \sigma_s^2)^\top (\sigma_s^1 - \sigma_s^2)]) ds \\ &\quad + \int_0^t 2(Y_s^1 - Y_s^2)^\top (\sigma_s^1 - \sigma_s^2)dW_s \\ &\quad + \int_0^t 2(Y_s^1 - Y_s^2)^\top [\nu(Y_s^1)dL_s^1 - \nu(Y_s^2)dL_s^2]. \end{aligned} \quad (3.14)$$

Then, for the product, Ito's formula yields

$$\begin{aligned} &\exp\{-2c(g_t^1 + g_t^2)\}|Y_t^1 - Y_t^2|^2 \\ &= 2 \int_0^t \exp\{-2c(g_s^1 + g_s^2)\}(Y_s^1 - Y_s^2)^\top [(b_s^1 - b_s^2)ds + (\sigma_s^1 - \sigma_s^2)dW_s + \nu(Y_s^1)dL_s^1 \\ &\quad - \nu(Y_s^2)dL_s^2] + \int_0^t \exp\{-2c(g_s^1 + g_s^2)\}\text{tr}[(\sigma_s^1 - \sigma_s^2)^\top (\sigma_s^1 - \sigma_s^2)]ds \\ &\quad - 2c \int_0^t |Y_s^1 - Y_s^2|^2 \exp\{-2c(g_s^1 + g_s^2)\}[\tilde{b}_s ds + \tilde{\sigma}_s^\top dW_s + dL_s^1 + dL_s^2] \\ &\quad + 2c^2 \int_0^t \exp\{-2c(g_s^1 + g_s^2)\}|Y_s^1 - Y_s^2|^2 \tilde{\sigma}_s \tilde{\sigma}_s^\top ds \\ &\quad - 4c \int_0^t \exp\{-2c(g_s^1 + g_s^2)\}(Y_s^1 - Y_s^2)^\top (\sigma_s^1 - \sigma_s^2)\tilde{\sigma}_s^\top ds. \end{aligned} \quad (3.15)$$

From the uniform exterior sphere condition (3.4), we have

$$\begin{aligned} -c|Y_s^1 - Y_s^2|^2 + (Y_s^1 - Y_s^2)^\top \nu(Y_s^1) &\leq 0, \\ -c|Y_s^1 - Y_s^2|^2 + (Y_s^2 - Y_s^1)^\top \nu(Y_s^2) &\leq 0, \quad a.s. \end{aligned} \quad (3.16)$$

To ease the notation, we denote $\kappa(s) := \exp\{-2c(g_s^1 + g_s^2)\}$; note that κ is bounded since g is bounded. Then,

$$\begin{aligned} \kappa(t)|Y_t^1 - Y_t^2|^2 &\leq 2 \int_0^t \kappa(s)(Y_s^1 - Y_s^2)^\top [(b_s^1 - b_s^2)ds + (\sigma_s^1 - \sigma_s^2)dW_s] \\ &\quad + \int_0^t \kappa(s)\text{tr}[(\sigma_s^1 - \sigma_s^2)^\top (\sigma_s^1 - \sigma_s^2)]ds \\ &\quad - 2c \int_0^t |Y_s^1 - Y_s^2|^2 \kappa(s)[\tilde{b}_s ds + \tilde{\sigma}_s^\top dW_s] \\ &\quad + 2c^2 \int_0^t \kappa(s)|Y_s^1 - Y_s^2|^2 \tilde{\sigma}_s \tilde{\sigma}_s^\top ds \\ &\quad - 4c \int_0^t \kappa(s)(Y_s^1 - Y_s^2)^\top (\sigma_s^1 - \sigma_s^2) \tilde{\sigma}_s^\top ds. \end{aligned} \quad (3.17)$$

Squaring both sides and applying the Cauchy–Schwarz inequality twice, we obtain for some constant $K > 0$

$$\begin{aligned} |Y_t^1 - Y_t^2|^4 &\leq K \left[\int_0^t [(Y_s^1 - Y_s^2)^\top (b_s^1 - b_s^2)]^2 ds + \int_0^t [\text{tr}[(\sigma_s^1 - \sigma_s^2)^\top (\sigma_s^1 - \sigma_s^2)]]^2 ds \right. \\ &\quad + \int_0^t |Y_s^1 - Y_s^2|^4 ds + \int_0^t [(Y_s^1 - Y_s^2)^\top (\sigma_s^1 - \sigma_s^2) \tilde{\sigma}_s^\top]^2 ds \\ &\quad + \left(\int_0^t \kappa(s)(Y_s^1 - Y_s^2)^\top (\sigma_s^1 - \sigma_s^2) dW_s \right)^2 \\ &\quad \left. + \left(\int_0^t \kappa(s)|Y_s^1 - Y_s^2|^2 \tilde{\sigma}_s dW_s \right)^2 \right], \end{aligned} \quad (3.18)$$

where we use the fact that $\kappa(s)$ is bounded by definition, and \tilde{b} and $\tilde{\sigma}$ are bounded on \bar{G} . Then, taking the supremum over $[0, t]$ and taking expectation, we get

$$\begin{aligned} \mathbb{E} \sup_{u \leq t} |Y_u^1 - Y_u^2|^4 &\leq K \left[\mathbb{E} \sup_{u \leq t} \left(\int_0^u [(Y_s^1 - Y_s^2)^\top (b_s^1 - b_s^2)]^2 ds \right. \right. \\ &\quad + \int_0^u [\text{tr}[(\sigma_s^1 - \sigma_s^2)^\top (\sigma_s^1 - \sigma_s^2)]]^2 ds \\ &\quad + \int_0^u |Y_s^1 - Y_s^2|^4 ds + \int_0^u [(Y_s^1 - Y_s^2)^\top (\sigma_s^1 - \sigma_s^2) \tilde{\sigma}_s^\top]^2 ds \Big) \\ &\quad + \mathbb{E} \sup_{u \leq t} \left(\int_0^u \kappa(s)(Y_s^1 - Y_s^2)^\top (\sigma_s^1 - \sigma_s^2) dW_s \right)^2 \\ &\quad \left. + \mathbb{E} \sup_{u \leq t} \left(\int_0^u \kappa(s)|Y_s^1 - Y_s^2|^2 \tilde{\sigma}_s dW_s \right)^2 \right]. \end{aligned} \quad (3.19)$$

The Riemann integrals have non-negative integrands so their supremum is reached at t . Meanwhile, we use Doob's inequality, which yields

$$\begin{aligned} \mathbb{E} \sup_{u \leq t} |Y_u^1 - Y_u^2|^4 &\leq K \mathbb{E} \left(\int_0^t [(Y_s^1 - Y_s^2)^\top (b_s^1 - b_s^2)]^2 ds \right. \\ &\quad + \int_0^t [\text{tr}[(\sigma_s^1 - \sigma_s^2)^\top (\sigma_s^1 - \sigma_s^2)]]^2 ds \\ &\quad + \int_0^t |Y_s^1 - Y_s^2|^4 ds + \int_0^t [(Y_s^1 - Y_s^2)^\top (\sigma_s^1 - \sigma_s^2) \tilde{\sigma}_s^\top]^2 ds \\ &\quad \left. + \int_0^t |(Y_s^1 - Y_s^2)^\top (\sigma_s^1 - \sigma_s^2)|^2 ds + \int_0^t |Y_s^1 - Y_s^2|^4 ds \right), \quad (3.20) \end{aligned}$$

where again we have used boundedness of $\kappa(s)$ and $\tilde{\sigma}$. Now using the Cauchy–Schwarz inequality and Assumption 3.2, we obtain

$$\begin{aligned} \mathbb{E} \sup_{u \leq t} |Y_u^1 - Y_u^2|^4 &\leq K \mathbb{E} \left(\int_0^t |Y_s^1 - Y_s^2|^2 |b_s^1 - b_s^2|^2 + |Y_s^1 - Y_s^2|^2 |\sigma_s^1 - \sigma_s^2|^2 \right. \\ &\quad \left. + |Y_s^1 - Y_s^2|^4 + |\sigma_s^1 - \sigma_s^2|^4 ds \right) \quad (3.21) \end{aligned}$$

$$\leq K \left(\int_0^t \mathbb{E} |Y_s^1 - Y_s^2|^4 + \mathcal{W}_4^4(\mu_s^1, \mu_s^2) ds \right). \quad (3.22)$$

Note that $|(Y_s^1 - Y_s^2)^\top (\sigma_s^1 - \sigma_s^2) \tilde{\sigma}_s^\top| \leq K |Y_s^1 - Y_s^2| |\sigma_s^1 - \sigma_s^2|$ follows from application of the Cauchy–Schwarz inequality, the operator norm being bounded by Frobenius norm, and $\tilde{\sigma}$ being bounded. Then,

$$\mathbb{E} \sup_{u \leq t} |Y_u^1 - Y_u^2|^4 \leq \int_0^t K \mathbb{E} \sup_{u \leq s} |Y_u^1 - Y_u^2|^4 ds + K \int_0^t \mathcal{W}_4^4(\mu_s^1, \mu_s^2) ds, \quad (3.23)$$

to which Grönwall's lemma can be applied to yield

$$\mathbb{E} \sup_{u \leq t} |Y_u^1 - Y_u^2|^4 \leq K e^{Kt} \int_0^t \mathcal{W}_4^4(\mu_s^1, \mu_s^2) ds. \quad (3.24)$$

Hence

$$D_T^4(\Phi(\mu^1), \Phi(\mu^2)) \leq \mathbb{E} \sup_{u \leq T} |Y_u^1 - Y_u^2|^4 \quad (3.25)$$

$$\leq K e^{KT} \int_0^T \mathcal{W}_4^4(\mu_u^1, \mu_u^2) du \quad (3.26)$$

$$\leq K e^{KT} \int_0^T D_u^4(\mu^1, \mu^2) du. \quad (3.27)$$

The inequality (3.25) follows from the definition of the metric D_T , while (3.27) is a consequence of $\mathcal{W}_4^4(\mu_u^1, \mu_u^2) \leq D_u^4(\mu^1, \mu^2)$. Lemma 3.1 is proved. \square

Now, we are ready to prove Theorem 3.1.

Proof of Theorem 3.1. Applying (3.8) twice yields

$$D_T^4(\Phi(\mu^1), \Phi(\mu^2)) \leq K_T \int_0^T D_{t_1}^4(\Phi(\mu^1), \Phi(\mu^2)) dt_1 \quad (3.28)$$

$$\leq K_T^2 \int_0^T \int_0^{t_1} D_{t_2}^4(\mu^1, \mu^2) dt_2 dt_1. \quad (3.29)$$

Continuing in this way for the j -fold composition Φ^j , we obtain

$$D_T^4(\Phi^j(\mu^1), \Phi^j(\mu^2)) \leq K_T^j \int_0^T \int_0^{t_1} \cdots \int_0^{t_{j-1}} D_{t_j}^4(\mu^1, \mu^2) dt_j \cdots dt_1. \quad (3.30)$$

Changing the order of integration yields

$$\begin{aligned} D_T^4(\Phi^j(\mu^1), \Phi^j(\mu^2)) &\leq K_T^j \int_0^T \int_{t_j}^T \cdots \int_{t_2}^T D_{t_j}^4(\mu^1, \mu^2) dt_1 \cdots dt_j \\ &= K_T^j \int_0^T \frac{(T - t_j)^{j-1}}{(j-1)!} D_{t_j}^4(\mu^1, \mu^2) dt_j \leq \frac{(K_T T)^j}{j!} D_T^4(\mu^1, \mu^2). \end{aligned} \quad (3.32)$$

Hence, if we choose j large enough such that

$$\frac{(K_T T)^j}{j!} < 1,$$

it follows that Φ^j is a contraction and Φ has a unique fixed point, as required to complete the proof. \square

3.2. Well-posedness of the particle system

Now, we show well-posedness of the particle system (2.3).

Theorem 3.2. *Let Assumptions 3.1 and 3.2 hold. Then there exists a unique strong solution of the SDEs (2.3).*

Proof. For the sake of simplicity in presentation, we denote $X_s^{i,N} := X^{i,N}(s)$, $W_s^i := W^i(s)$ and $L_s^i := L^i(s)$. Let \mathbb{S} be the space of continuous and $\mathcal{F}_t^{\mathbf{W}}$ -adapted \bar{G}^N -valued processes. We define the map

$$\begin{aligned} \Phi : \mathbb{S} &\rightarrow \mathbb{S}, \\ Y &\mapsto \bar{Y}, \end{aligned} \quad (3.33)$$

where $\bar{Y} = (\bar{Y}^{1,N^\top}, \dots, \bar{Y}^{N,N^\top})^\top$ is the solution to

$$\begin{aligned} \bar{Y}_t^{i,N} &= X_0^{i,N} + \int_0^t b(s, \bar{Y}_s^{i,N}, \hat{\mu}_{Y_s}) ds + \int_0^t \sigma(s, \bar{Y}_s^{i,N}, \hat{\mu}_{Y_s}) dW_s^i \\ &\quad + \int_0^t \nu(\bar{Y}_s^{i,N}) dL_s^{i,N}, \quad i = 1, \dots, N, \end{aligned} \quad (3.34)$$

and $\hat{\mu}_{Y_t}$ is the empirical measure of an input process $Y \in \mathbb{S}$ at time t (see (2.2)). The SDE (3.34) is a reflected SDE with random coefficients. Existence and uniqueness of each component \bar{Y}^i follow from Theorem 2.2 in Ref. 12. Hence, the map Φ is well-defined.

Let $Y^{(1)}, Y^{(2)} \in \mathbb{S}$ and $\bar{Y}^{(j)} = \Phi(Y^{(j)})$, $j = 1, 2$. Applying the technique of Lemma 3.1 to each of the N components of the two processes $\bar{Y}^{(j)}$, $j = 1, 2$, we obtain (cf. (3.22))

$$\mathbb{E} \sup_{u \leq t} |\bar{Y}_u^{(1), i, N} - \bar{Y}_u^{(2), i, N}|^4 \leq K \left(\int_0^t \mathbb{E} |\bar{Y}_s^{(1), i, N} - \bar{Y}_s^{(2), i, N}|^4 + \mathbb{E} \mathcal{W}_4^4(\hat{\mu}_{Y_s^{(1)}}, \hat{\mu}_{Y_s^{(2)}}) ds \right), \quad (3.35)$$

for $i = 1, \dots, N$. Applying Grönwall's lemma yields

$$\mathbb{E} \sup_{u \leq t} |\bar{Y}_u^{(1), i, N} - \bar{Y}_u^{(2), i, N}|^4 \leq K e^{Kt} \left(\int_0^t \mathbb{E} \mathcal{W}_4^4(\hat{\mu}_{Y_s^{(1)}}, \hat{\mu}_{Y_s^{(2)}}) ds \right). \quad (3.36)$$

From (3.2) and (2.2), it can be seen that

$$\mathbb{E} \mathcal{W}_4^4(\hat{\mu}_{Y_s^{(1)}}, \hat{\mu}_{Y_s^{(2)}}) \leq \frac{1}{N} \sum_{i=1}^N \mathbb{E} |Y_s^{(1), i, N} - Y_s^{(2), i, N}|^4. \quad (3.37)$$

Hence,

$$\mathbb{E} \sup_{u \leq t} |\bar{Y}_u^{(1)} - \bar{Y}_u^{(2)}|^4 \leq K \sum_{i=1}^N \mathbb{E} \sup_{u \leq t} |\bar{Y}_u^{(1), i, N} - \bar{Y}_u^{(2), i, N}|^4 \quad (3.38)$$

$$\leq K e^{Kt} \int_0^t \sum_{i=1}^N \mathbb{E} |Y_s^{(1), i, N} - Y_s^{(2), i, N}|^4 ds \quad (3.39)$$

$$\leq K e^{Kt} \int_0^t \mathbb{E} \sup_{u \leq s} |Y_u^{(1)} - Y_u^{(2)}|^4 ds, \quad (3.40)$$

where for the second inequality we use (3.36) and then (3.37). One can then show that the map Φ is a contraction as before, see (3.32). The unique fixed-point of Φ is the solution to the particle system. \square

3.3. Well-posedness of the CBO models

We now verify that the CBO mean-field SDEs and their particle approximations from Sec. 2.2 satisfy Assumption 3.2 so that their well-posedness is established.

For $\mu \in \mathcal{P}(\bar{G})$, let us define

$$\bar{X}^\mu := \frac{\int_{\bar{G}} x e^{-\alpha f(x)} \mu(dx)}{\int_{\bar{G}} e^{-\alpha f(x)} \mu(dx)}. \quad (3.41)$$

The following lemma is proved in Ref. 13.

Lemma 3.2. *Let Assumption 3.1 hold and f satisfy Assumption 2.1. There exists $K > 0$ such that for all $\mu, \bar{\mu} \in \mathcal{P}(\bar{G})$,*

$$|\bar{X}^\mu - \bar{X}^{\bar{\mu}}| \leq K\mathcal{W}_2(\mu, \bar{\mu}). \quad (3.42)$$

Now, we show that the coefficients of the CBO model (2.12) satisfy Assumption 2.1.

Lemma 3.3. *The coefficients of (2.12),*

$$b(t, x, \mu) = \beta(x - \bar{X}^\mu) \quad \text{and} \quad \sigma(t, x, \mu) = \sigma \text{Diag}(x - \bar{X}^\mu), \quad (3.43)$$

are Lipschitz, uniformly in time, with respect to the space and measure arguments (i.e. they satisfy Assumption 3.2).

Proof. For $x, \bar{x} \in \mathbb{R}^d$ and $\mu, \bar{\mu} \in \mathcal{P}(\bar{G})$,

$$\begin{aligned} & |b(t, x, \mu) - b(t, \bar{x}, \bar{\mu})| + |\sigma(t, x, \mu) - \sigma(t, \bar{x}, \bar{\mu})| \\ &= \beta|(x - \bar{x}) + (\bar{X}^{\bar{\mu}} - \bar{X}^\mu)| + \sigma|(x - \bar{x}) + (\bar{X}^{\bar{\mu}} - \bar{X}^\mu)| \\ &\leq K(|x - \bar{x}| + |\bar{X}^\mu - \bar{X}^{\bar{\mu}}|) \leq K(|x - \bar{x}| + \mathcal{W}_2(\mu, \bar{\mu})) \leq K(|x - \bar{x}| + \mathcal{W}_4(\mu, \bar{\mu})), \end{aligned}$$

by application of Lemma 3.2. \square

Hence, by Theorem 3.1, we have well-posedness of the mean-field limit (2.12) and the particle system (2.14). In the same way it can be verified that the coefficients of the CBO model (2.16) satisfy Assumption 3.2, from which well-posedness of the mean-field limit (2.16) and the particle system (2.17) follows.

4. Convergence of Interacting Particle System to the Mean-Field Limit

In this section we prove a theorem on propagation of chaos with the optimal convergence rate. Let $\mathbf{X}(\mathbf{t}) := (X^1(t), \dots, X^N(t))^\top$, where $X^i(t)$, $i = 1, \dots, N$, are i.i.d. particles solving the McKean–Vlasov SDEs (2.1) which are driven by the independent Wiener processes W^i that are the same as in the particle system (2.3).

Under Assumptions 3.1 and 3.2, it is not difficult to prove using an analogue of (3.22) and the well-known result for rates of convergence of empirical measures (see Theorem 1 in Ref. 25) that for some constant $C > 0$:

$$\max_{i=1, \dots, N} \sup_{t \leq T} \mathbb{E}|X^{i,N}(t) - X^i(t)|^4 \leq C \begin{cases} N^{-1/2}, & d < 8, \\ N^{-1/2} \log N, & d = 8, \\ N^{-\frac{4}{d}}, & d > 8. \end{cases} \quad (4.1)$$

Under Assumption 4.1 replacing Assumption 3.2, we instead prove the optimal convergence rate of order $1/\sqrt{N}$ for any d . The CBO models from Secs. 2.2.1 and 2.2.2 satisfy Assumption 4.1.

Assumption 4.1. There exist a constant $L > 0$ and functions $\phi_j(t, x, y)$, $j = 1, \dots, J$, continuous on $[0, T] \times \bar{G} \times \bar{G}$ satisfying for some $C > 0$

$$|\phi_j(t, x, y) - \phi_j(t, x, z)| \leq C|y - z|$$

such that for any $x, y \in \bar{G}$ and any $\mu_1, \mu_2 \in \mathcal{P}(\bar{G})$

$$\begin{aligned} & |b(t, x, \mu_1) - b(t, y, \mu_2)| + |\sigma(t, x, \mu_1) - \sigma(t, y, \mu_2)| \\ & \leq L \left(|x - y| + \sum_{j=1}^J \left| \int_G \phi_j(t, x, z) d\mu_1(z) - \int_G \phi_j(t, x, z) d\mu_2(z) \right| \right). \end{aligned} \quad (4.2)$$

Also, the coefficients $b(t, x, \mu)$ and $\sigma(t, x, \mu)$ are continuous in t .

Remark 4.1. Using the duality form for the Wasserstein 1-metric \mathcal{W}_1 , the assumption (4.2) can be expressed as

$$|b(t, x, \mu_1) - b(t, y, \mu_2)| + |\sigma(t, x, \mu_1) - \sigma(t, y, \mu_2)| \leq L(|x - y| + \mathcal{W}_1(\mu_1, \mu_2))$$

with a different $L > 0$.

We will need the following elementary lemma.

Lemma 4.1. Let $\{A^i\}_{i=1}^N$ be a collection of independent \mathbb{R}^d -valued random variables with fourth bounded moment and $\mathbb{E}(A^i) = 0$, $i = 1, \dots, N$. Then

$$\mathbb{E} \left| \frac{1}{N} \sum_{i=1}^N A^i \right|^4 \leq \frac{C}{N^2}, \quad (4.3)$$

where $C > 0$ is independent of N .

Let us prove the following auxiliary lemma.

Lemma 4.2. Let Assumptions 3.1 and 4.1 be satisfied. Then the following bounds hold. For all $i = 1, \dots, N$,

$$\begin{aligned} & \mathbb{E}|b(t, X^{i,N}(t), \hat{\mu}_{\mathbf{X}^N(t)}) - b(t, X^i(t), \hat{\mu}_{\mathbf{X}(t)})|^4 \\ & + \mathbb{E}|\sigma(t, X^{i,N}(t), \hat{\mu}_{\mathbf{X}^N(t)}) - \sigma(t, X^i(t), \hat{\mu}_{\mathbf{X}(t)})|^4 \\ & \leq C \left(\mathbb{E}|X^{i,N}(t) - X^i(t)|^4 + \frac{1}{N} \sum_{j=1}^N \mathbb{E}|X^{j,N}(t) - X^j(t)|^4 \right), \end{aligned} \quad (4.4)$$

where $C > 0$ is independent of N .

For all $i = 1, \dots, N$,

$$\begin{aligned} & \mathbb{E}|b(t, X^i(t), \hat{\mu}_{\mathbf{X}(t)}) - b(t, X^i(t), \mathcal{L}_t^X)|^4 \\ & + \mathbb{E}|\sigma(t, X^i(t), \hat{\mu}_{\mathbf{X}(t)}) - \sigma(t, X^i(t), \mathcal{L}_t^X)|^4 \leq \frac{C}{N^2}, \end{aligned} \quad (4.5)$$

where $C > 0$ is independent of N .

Proof. Thanks to Assumption 4.1, we obtain

$$\begin{aligned} & \mathbb{E}|b(t, X^{i,N}(t), \hat{\mu}_{\mathbf{X}^N(t)}) - b(t, X^i(t), \hat{\mu}_{\mathbf{X}(t)})|^4 \\ & \quad + \mathbb{E}|\sigma(t, X^{i,N}(t), \hat{\mu}_{\mathbf{X}^N(t)}) - \sigma(t, X^i(t), \hat{\mu}_{\mathbf{X}(t)})|^4 \\ & \leq C\mathbb{E}|X^{i,N}(t) - X^i(t)|^4 \\ & \quad + C \sum_{j=1}^J \mathbb{E} \left| \frac{1}{N} \sum_{l=1}^N \phi_j(t, X^i(t), X^{l,N}(t)) - \frac{1}{N} \sum_{l=1}^N \phi_j(t, X^i(t), X^l(t)) \right|^4 \\ & \leq C\mathbb{E}|X^{i,N}(t) - X^i(t)|^4 + C \frac{1}{N} \sum_{l=1}^N \mathbb{E}|X^{l,N}(t) - X^l(t)|^4, \end{aligned}$$

hence we arrived at (4.4).

Thanks to Assumption 4.1, we get

$$\begin{aligned} & \mathbb{E}|b(t, X^i(t), \hat{\mu}_{\mathbf{X}(t)}) - b(t, X^i(t), \mathcal{L}_t^X)|^4 + \mathbb{E}|\sigma(t, X^i(t), \hat{\mu}_{\mathbf{X}(t)}) - \sigma(t, X^i(t), \mathcal{L}_t^X)|^4 \\ & \leq C \sum_{j=1}^J \mathbb{E} \left| \frac{1}{N} \sum_{l=1}^N \phi_j(t, X^i(t), X^l(t)) - \int_G \phi_j(t, X^i(t), y) \mathcal{L}_t^X(dy) \right|^4 \\ & \leq C \sum_{j=1}^J \mathbb{E} \left| \frac{1}{N} \sum_{l=1}^N \phi_j(t, X^i(t), X^l(t)) - \frac{1}{N-1} \sum_{l=1, l \neq i}^N \phi_j(t, X^i(t), X^l(t)) \right|^4 \\ & \quad + C \sum_{j=1}^J \mathbb{E} \left| \frac{1}{N-1} \sum_{l=1, l \neq i}^N \phi_j(t, X^i(t), X^l(t)) - \int_G \phi_j(t, X^i(t), y) \mathcal{L}_t^X(dy) \right|^4 \\ & \leq \frac{C}{N^4} + C \sum_{j=1}^J \mathbb{E} \left(\mathbb{E} \left(\left| \frac{1}{N-1} \sum_{l=1, l \neq i}^N \phi_j(t, x, X^l(t)) \right. \right. \right. \\ & \quad \left. \left. \left. - \int_G \phi_j(t, x, y) \mathcal{L}_t^X(dy) \right|^4 \middle| X^i(t) = x \right) \right). \end{aligned}$$

Note that for each j

$$D_j^l(x) := \phi_j(t, x, X^l(t)) - \int_G \phi_j(t, x, y) \mathcal{L}_t^X(dy), \quad l = 1, \dots, N, \quad (4.6)$$

are independent random variables with bounded moments and $\mathbb{E}D_j^l(x) = 0$. Then, applying a conditional version of Lemma 4.1, we arrive at (4.5). \square

Now, we proceed to the propagation of chaos theorem.

Theorem 4.1. *Let Assumptions 3.1 and 4.1 be satisfied. Then the following bound holds:*

$$\left(\max_{i=1, \dots, N} \mathbb{E} \sup_{u \leq t} |X^{i,N}(u) - X^i(u)|^4 \right)^{1/4} \leq \frac{C}{N^{1/2}}, \quad (4.7)$$

where $X^{i,N}$ represents the i th particle among the interacting particles driven by (2.3); X^i , $i = 1, \dots, N$, are independent and identical copies of (2.1) with each X^i being driven by the same Wiener processes as the corresponding $X^{i,N}$; and $C > 0$ is a constant independent of N .

Proof. For brevity, we write $X_t^{i,N} := X^{i,N}(t)$ and $X_t^i := X^i(t)$. Analogously to how (3.21) was derived, we can get

$$\begin{aligned} \mathbb{E} \sup_{u \leq t} |X_u^{i,N} - X_u^i|^4 &\leq K \mathbb{E} \left(\int_0^t |X_s^{i,N} - X_s^i|^2 |b(s, X_s^{i,N}, \hat{\mu}_{\mathbf{X}_s^N}) - b(s, X_s^i, \mathcal{L}_s^X)|^2 \right. \\ &\quad + |X_s^{i,N} - X_s^i|^2 |\sigma(s, X_s^{i,N}, \hat{\mu}_{\mathbf{X}_s^N}) - \sigma(s, X_s^i, \mathcal{L}_s^X)|^2 \\ &\quad \left. + |X_s^{i,N} - X_s^i|^4 + |\sigma(s, X_s^{i,N}, \hat{\mu}_{\mathbf{X}_s^N}) - \sigma(s, X_s^i, \mathcal{L}_s^X)|^4 ds \right). \end{aligned} \quad (4.8)$$

We have

$$\begin{aligned} |b(s, X_s^{i,N}, \hat{\mu}_{\mathbf{X}_s^N}) - b(s, X_s^i, \mathcal{L}_s^X)|^4 &\leq 4(|b(s, X_s^{i,N}, \hat{\mu}_{\mathbf{X}_s^N}) - b(s, X_s^i, \hat{\mu}_{\mathbf{X}_s})|^4 \\ &\quad + |b(s, X_s^i, \hat{\mu}_{\mathbf{X}_s}) - b(s, X_s^i, \mathcal{L}_s^X)|^4), \end{aligned} \quad (4.9)$$

$$\begin{aligned} |\sigma(s, X_s^{i,N}, \hat{\mu}_{\mathbf{X}_s^N}) - \sigma(s, X_s^i, \mathcal{L}_s^X)|^4 &\leq 4(|\sigma(s, X_s^{i,N}, \hat{\mu}_{\mathbf{X}_s^N}) - \sigma(s, X_s^i, \hat{\mu}_{\mathbf{X}_s})|^4 \\ &\quad + |\sigma(s, X_s^i, \hat{\mu}_{\mathbf{X}_s}) - \sigma(s, X_s^i, \mathcal{L}_s^X)|^4). \end{aligned} \quad (4.10)$$

Using Young's inequality, (4.9), (4.10) and Lemma 4.2, we obtain from (4.8):

$$\begin{aligned} \mathbb{E} \sup_{u \leq t} |X_u^{i,N} - X_u^i|^4 &\leq C \int_0^t \mathbb{E} |X^{i,N}(s) - X^i(s)|^4 \\ &\quad + \frac{1}{N} \sum_{j=1}^N \mathbb{E} |X^{j,N}(s) - X^j(s)|^4 ds + C \frac{1}{N^2}. \end{aligned}$$

Hence

$$\max_{i=1, \dots, N} \mathbb{E} \sup_{u \leq t} |X_u^{i,N} - X_u^i|^4 \leq C \int_0^t \max_{i=1, \dots, N} \mathbb{E} \sup_{u \leq s} |X^{i,N}(u) - X^i(u)|^4 ds + C \frac{1}{N^2},$$

which after applying Grönwall's lemma gives the desired result. \square

It is not difficult to verify that the CBO models from Secs. 2.2.1 and 2.2.2 satisfy Assumption 4.1. Consequently, we get the following corollary.

Corollary 4.1. *The particle systems (2.14) and (2.17) converge to their mean-field limits (2.12) and (2.16), respectively: for them the inequality (4.7) holds.*

5. Long-Time Behavior of Reflected Mean-Field Models

In Sec. 5.1, we use the coupling technique to study long time behavior of the reflected McKean–Vlasov SDEs (2.1) with $\sigma \equiv I$. In Sec. 5.2, we show convergence of the CBO models from Sec. 2.2 towards the global minimum.

5.1. Convergence of reflected mean-field SDEs with additive noise

Consider the reflected McKean–Vlasov SDEs (2.1) with $\sigma \equiv I$:

$$dX(t) = b(X(t), \mathcal{L}_{X(t)})dt + dW(t) + \nu(X(t))dL(t), \quad X(0) \in \bar{G}. \quad (5.1)$$

Here, we provide a quantitative non-asymptotic bound for the exponential convergence of $\mathcal{L}_{X(t)}$, i.e. the law of $X(t)$, to the invariant measure $\tilde{\mu}$ defined on \bar{G} .

Recall $c := 1/(2R_0)$ where R_0 is the radius of uniform exterior sphere (see (3.4)). We denote

$$R_1 = \sup_{x, y \in \bar{G}} |x - y| \quad \text{and} \quad \hat{\lambda}_c = 1 - 2cR_1. \quad (5.2)$$

Note that for a convex domain $c = 0$.

Assumption 5.1. The constant $\hat{\lambda}_c > 0$.

This assumption allows for the domain G to be non-convex but it is weaker than the uniform exterior sphere condition (3.4).

As in the proof of Lemma 3.1, $d(\cdot, \partial G)$ is the distance to the boundary of G , defined on some neighborhood of ∂G within G and the function $g(\cdot)$ is a smooth, bounded extension of $d(\cdot, \partial G)$ to the whole space so that

$$\max_{x \in \bar{G}} |\nabla g(x)| = 1. \quad (5.3)$$

We also use the notation

$$g_{\min} = \min_{x \in \bar{G}} g(x) \quad \text{and} \quad g_{\max} = \max_{x \in \bar{G}} g(x). \quad (5.4)$$

We employ reflection coupling (see Refs. 45, 20 and 23) to establish a 1-Wasserstein bound between the law of $X(t)$ and its invariant measure. Using reflection coupling, the convex domain case was considered in Remark 3 in Ref. 23 for additive noise and in Ref. 70 for multiplicative noise.

Theorem 5.1. *Let Assumptions 3.1, 4.1 and 5.1 hold. Then the following bound for the solution of (5.1) holds:*

$$\mathcal{W}_1(\mathcal{L}_{X(t)}, \tilde{\mu}) \leq C_{mf} \mathcal{W}_1(\mathcal{L}_{X(0)}, \tilde{\mu}) e^{-C_0 t}, \quad (5.5)$$

where

$$C_{mf} = 2 \exp \left(\frac{K_1}{K_3} \frac{R_1^2}{2} + \frac{K_2}{K_3} R_1 \right) \exp(2cg_{\max}), \quad (5.6)$$

$$C_0 = \frac{K_3}{2 \int_0^{R_1} \int_0^r \exp(\frac{K_1}{K_3} \frac{r^2 - s^2}{2} + \frac{K_2}{K_3} (r - s)) ds dr},$$

with

$$K_1 = L + c \sup_{x \in \bar{G}, \mu \in \mathcal{P}(\bar{G})} (2|b(x, \mu)| + |\Delta g(x)|) + 2c^2, \quad (5.7)$$

$$K_2 = 4ce^{-2cg_{\min}} + LR_1e^{-2cg_{\min}}, \quad K_3 = 2\hat{\lambda}_ce^{-4cg_{\max}},$$

and L is from (4.2).

Proof. Consider the coupling

$$dX(t) = b(X(t), \mathcal{L}_{X(t)})dt + dW(t) + \nu(X(t))dL^X(t), \quad t > 0, \quad (5.8)$$

$$dY(t) = b(Y(t), \mathcal{L}_{Y(t)})dt + (I - 2E(t)E^\top(t))dW(t) + \nu(Y(t))dL^Y(t), \quad \tau > t, \quad (5.9)$$

and

$$X(t) = Y(t), \quad \tau \leq t,$$

where the coupling time τ is

$$\tau := \inf\{t > 0; X(t) = Y(t)\}, \quad (5.10)$$

and $E(t) = (X(t) - Y(t))/|X(t) - Y(t)|$. Note that for every $s \geq 0$ the matrix $I - 2E(t)E^\top(t)I(\tau > t)$ is orthogonal.

In what follows, for brevity, we will denote $X_t := X(t)$, $Y_t := Y(t)$, $W_t := W(t)$, $L_t^X := L^X(t)$, $L_t^Y := L^Y(t)$, $E_t := E(t)$, $b_t^X := b(X_t, \mathcal{L}_{X_t})$, and $b_t^Y := b(Y_t, \mathcal{L}_{Y_t})$. Denote $Z_t := g(X_t) + g(Y_t)$. Introduce $r_t = \exp(-cZ_t)|X_t - Y_t|I(\tau > t)$.

By Ito's formula, we have for $\tau > t$:

$$\begin{aligned} dr_t = \exp(-cZ_t) \Big[& (E_t \cdot (b_t^X - b_t^Y))dt + 2E_t^\top dW_t + |X_t - Y_t|[cF_tdt \\ & + \frac{c^2}{2}H_tdt - c(\nabla g(X_t) \cdot dW_t) - c(\nabla g(Y_t) \cdot (I - 2E_tE_t^\top)dW_t)] \\ & - 2c\nabla^\top g(X_t)E_tdt + 2c\nabla^\top g(Y_t)E_tdt + \{((E_t \cdot \nu(X_t)) - c|X_t - Y_t|)dL_t^X \\ & - ((E_t \cdot \nu(Y_t)) + c|X_t - Y_t|)dL_t^Y\} \Big], \end{aligned}$$

where $F_t := -[(\nabla g(X_t) \cdot b_t^X) + (\nabla g(Y_t) \cdot b_t^Y) + \frac{1}{2}\Delta g(X_t) + \frac{1}{2}\Delta g(Y_t)]$ and $H_t := |\nabla g(X_t) + (I - 2E_tE_t^\top)\nabla g(Y_t)|^2$.

Consider an increasing concave function $\psi : [0, R_1] \rightarrow \mathbb{R}_+$ with $\psi(0) = 0$, whose precise choice will be made later. Using Ito's formula, we get for $\tau > t$:

$$d\psi(r_t) = \psi'(r_t)dr_t + \frac{1}{2}\psi''(r_t)d[r, r]_t,$$

where $[r, r]_t$ denotes a bracket process which is a non-decreasing process satisfying for $\tau > t$:

$$d[r_t, r_t] = e^{-2cZ_t} | -c|X_t - Y_t|\nabla g(X_t) - c|X_t - Y_t|(I - 2E_tE_t^\top)\nabla g(Y_t) + 2E_t|^2 dt$$

$$\begin{aligned}
 &= 4e^{-2cZ_t} dt + e^{-2cZ_t} c^2 |X_t - Y_t|^2 |\nabla g(X_t) + (I - 2E_t E_t^\top) \nabla g(Y_t)|^2 \\
 &\quad - 4|X_t - Y_t| c e^{-2cZ_t} ((\nabla g(X_t) \cdot E_t) - (\nabla g(Y_t) \cdot E_t)) dt \\
 &\geq 4e^{-2cZ_t} dt - 4e^{-2cZ_t} c ((\nabla g(X_t) - \nabla g(Y_t)) \cdot (X_t - Y_t)) dt \\
 &\geq 4e^{-2cZ_t} (1 - 2cR_1) dt = 4e^{-2cZ_t} \hat{\lambda}_c dt.
 \end{aligned} \tag{5.11}$$

Let $F_{\max} := \sup_{x \in \bar{G}, \mu \in \mathcal{P}(\bar{G})} (2|b(x, \mu)| + |\Delta g(x)|)$. Using (3.4) and that $\max_{x \in \bar{G}} |\nabla g(x)| = 1$, $\psi' > 0$ and $\psi'' < 0$, we get for $\tau > t$:

$$\begin{aligned}
 d\psi(r_t) &\leq \psi'(r_t) \exp(-cZ_t) |b_t^X - b_t^Y| dt + c\psi'(r_t) r_t (F_{\max} + 2c) dt \\
 &\quad + 4c \exp(-cZ_t) \psi'(r_t) dt \\
 &\quad + 2\hat{\lambda}_c \psi''(r_t) \exp(-2cZ_t) dt + \psi'(r_t) \exp(-cZ_t) (2(E_t \cdot dW_t) \\
 &\quad - c(\nabla g(X_t) \cdot dW_t) - c(\nabla g(Y_t) \cdot (I - 2E_t E_t^\top) dW_t)).
 \end{aligned}$$

Let us denote the martingale term for $\tau > t$ as

$$M_t = \int_0^t \psi'(r_u) \exp(-cZ_u) ((2E_u - c\nabla g(X_u) - c(I - 2E_u E_u^\top) \nabla g(Y_u)) \cdot dW_u).$$

Exploiting Assumption 4.1, we obtain

$$\begin{aligned}
 \mathbb{E}\psi(r_{t \wedge \tau}) &\leq \mathbb{E}\psi(r_0) + \mathbb{E}\left\{ \int_0^{t \wedge \tau} (\psi'(r_u) (Lr_u + \exp(-cZ_u) L\mathbb{E}|X_u - Y_u|) \right. \\
 &\quad + c\psi'(r_u) r_u (F_{\max} + 2c) + 4c \exp(-cZ_u) \psi'(r_u) \\
 &\quad \left. + 2\hat{\lambda}_c \psi''(r_u) \exp(-2cZ_u)) du \right\} + \mathbb{E}M_{t \wedge \tau} \\
 &\leq \mathbb{E}\psi(r_0) + \mathbb{E}\left\{ \int_0^{t \wedge \tau} \psi'(r_u) (K_1 r_u + K_2) + \psi''(r_u) K_3 du \right\},
 \end{aligned} \tag{5.12}$$

where we have used Doob's optional stopping theorem to get $\mathbb{E}M_{t \wedge \tau} = 0$.

Now, we aim to find an increasing concave function ψ such that for $r \in [0, R_1]$:

$$\psi'(r) (K_1 r + K_2) + K_3 \psi''(r) \leq -C_0 \psi(r), \tag{5.13}$$

for some constant $C_0 > 0$ independent of r . To this end, we make the choice of derivative of ψ inspired from Ref. 23 as:

$$\psi'(r) = \psi_1(r) \psi_2(r),$$

where

$$\psi_1(r) = \exp\left(-\frac{K_1}{K_3} \frac{r^2}{2} - \frac{K_2}{K_3} r\right)$$

and

$$\psi_2(r) = 1 - \frac{C_0}{K_3} \int_0^r \frac{1}{\psi_1(s)} \int_0^s \psi_1(s') ds' ds \tag{5.14}$$

with

$$C_0 = \frac{K_3}{2 \int_0^{R_1} \frac{1}{\psi_1(s)} \int_0^s \psi_1(s') ds' ds}.$$

It is not difficult to verify that $\psi(r) = \int_0^r \psi_1(s) \psi_2(s) ds$ satisfies (5.13). Further, $1/2 \leq \psi_2(r) \leq 1$ and hence

$$\frac{r}{2} \psi_1(R_1) \leq \psi(r) \leq r. \quad (5.15)$$

From (5.12) and (5.13), taking into account that $r(\tau) = 0$ and $\psi(0) = 0$, we get

$$\begin{aligned} \mathbb{E}(\psi(r_t) I(\tau \geq t)) &= \mathbb{E}\psi(r_{t \wedge \tau}) \leq \mathbb{E}\psi(r_0) - C_0 \mathbb{E} \int_0^{t \wedge \tau} \psi(r_u) du \\ &= \mathbb{E}\psi(r_0) - C_0 \int_0^t \mathbb{E}(\psi(r_u) I(\tau \geq t)) du. \end{aligned}$$

Therefore, $\mathbb{E}(\psi(r_t) I(\tau \geq t)) \leq \mathbb{E}\psi(r_0) e^{-C_0 t}$. Noting that $\mathbb{E}(\psi(r_{t \wedge \tau}) I(\tau \leq t)) = 0$, we have

$$\mathbb{E}\psi(r_t) \leq \mathbb{E}\psi(r_0) e^{-C_0 t}.$$

Then, thanks to (5.15), we get

$$\mathbb{E}r_t \leq 2\psi_1^{-1}(R_1) \mathbb{E}\psi(r_0) e^{-C_0 t} \quad (5.16)$$

and, since $\exp(-2cg_{\max})|X_t - Y_t| \leq r_t$, we arrive at

$$\mathbb{E}|X_t - Y_t| \leq 2 \exp(2cg_{\max}) \psi_1^{-1}(R_1) \mathbb{E}|X_0 - Y_0| e^{-C_0 t}. \quad \square$$

5.2. Convergence of mean-field limit of CBO-type models to the global minimum

This section is devoted to showing convergence of the constrained CBO models from Sec. 2.2 towards global minimizers. Similar to Refs. 13 and 16 (see also Ref. 38), the main tool which we will utilize is the Laplace principle which states that for any compactly supported measure μ and positive function f the following holds:

$$\lim_{\alpha \rightarrow \infty} -\frac{1}{\alpha} \log \int_{\mathbb{R}^d} e^{-\alpha f(x)} \mu(dx) = f(x_{\min}) \quad (5.17)$$

with x_{\min} being the minimizer of $f(x)$ defined on the support of μ . We will use the notation

$$f_{\text{osc}} = f_{\max} - f_{\min}.$$

The analysis in this section is done for convex domains.

Assumption 5.2. G is a convex bounded domain.

Let us explain why we restrict analysis in this section to convex domains. In the case of non-convex domains, CBO models with constraints of the type presented

in Secs. 2.2.1 and 2.2.2 face two difficulties. The first difficulty concerns the proof techniques used for showing convergence to the global minimum which have been used so far in the CBO literature (see, e.g. Refs. 13, 16, 38 and 4 and references therein and also the proofs below in this section). Roughly speaking, noise does not play a positive role within these proofs which rely on the drift driving solutions of the mean-field SDEs to the consensus. It works well in the convex case and in the whole Euclidean space. However, in situations like the one illustrated in Fig. 1, the drift forces trajectories to go outside the domain rather than driving it to a consensus and, hence, we need to rely on the noise term (via effectively large deviations) to get trajectories to a proximity of the global minimum, which happens with a positive probability, and then the drift can drive trajectories to a consensus. Hence, a probabilistic proof needs to be developed for proving convergence to the global minimum, which is an interesting problem for future research. Such a proof would also be able to provide more insight on how convergence to the global minimum depends on the noise strength which would be useful even in the whole Euclidean space. The second difficulty is more fundamental as it is related to the design of CBO models themselves. In the example of Fig. 1, the drift forces trajectories the wrong way because its form is based on the Euclidean metric. Therefore, it is of interest to find a different formulation of CBO models which imbibe more information of the domain (e.g. by using a non-Euclidean metric) but at the same time remain computationally efficient. Constructing such models is out of scope of this work. Nevertheless, we tested the CBO model of Sec. 2.2.1 on a non-convex function with non-convex domain (see Sec. 6.3) and the CBO model demonstrated excellent performance.

In Theorem 5.2, we prove convergence of the reflected CBO model from Sec. 2.2.1 towards the global minimum and consider the case of CBO with repelling force from Sec. 2.2.2 in Theorem 5.3. We note that under Assumptions 3.2 and 5.2 well-posedness of (2.1) and the corresponding propagation of chaos were proved in Ref. 1.

Theorem 5.2. *Let Assumptions 2.1 and 5.2 hold. If the following condition is satisfied*

$$\eta_0 := 2\beta - \sigma^2(1 + e^{2\alpha f_{osc}}) > 0$$

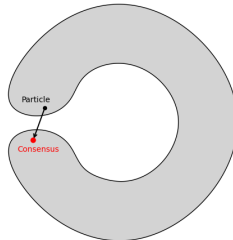


Fig. 1. The example of a non-convex domain, where the Euclidean path of a particle to the consensus does not lie within the domain. In the convex case, this behavior cannot occur.

then there exists an $x^* \in \bar{G}$ such that $X(t) \rightarrow x^*$ as $t \rightarrow \infty$ and

$$f(x^*) \leq f_{\min} + \Gamma(\alpha),$$

where $X(t)$ is the solution of the mean-field SDE (2.12) and $\Gamma(\alpha) \rightarrow 0$ as $\alpha \rightarrow \infty$.

Proof. Using Ito's formula, we get

$$\begin{aligned} |X(t) - \mathbb{E}X(t)|^2 &= |X(0) - \mathbb{E}X(0)|^2 - 2 \int_0^t \beta(X(s) - \mathbb{E}X(s)) \cdot (X(s) - \bar{X}(s)) ds \\ &\quad - 2 \int_0^t \beta(X(s) - \mathbb{E}X(s))^\top d\mathbb{E}X(s) \\ &\quad + 2 \int_0^t \sigma(X(s) - \mathbb{E}X(s)) \cdot \text{Diag}(X(s) - \bar{X}(s)) dW(s) \\ &\quad + \int_0^t \sigma^2 |X(s) - \bar{X}(s)|^2 ds + 2 \int_0^t (X(s) - \mathbb{E}X(s)) \cdot \nu(X(s)) dL(s) \\ &= |X(0) - \mathbb{E}X(0)|^2 - 2 \int_0^t \beta |X(s) - \mathbb{E}X(s)|^2 ds \\ &\quad - 2 \int_0^t \beta(X(s) - \mathbb{E}X(s))^\top d\mathbb{E}X(s) \\ &\quad - 2 \int_0^t \beta(X(s) - \mathbb{E}X(s)) \cdot (\mathbb{E}X(s) - \bar{X}(s)) ds \\ &\quad + \int_0^t \sigma^2 |X(s) - \bar{X}(s)|^2 ds \\ &\quad + 2 \int_0^t \sigma(X(s) - \mathbb{E}X(s)) \cdot \text{Diag}(X(s) - \bar{X}(s)) dW(s) \\ &\quad + 2 \int_0^t (X(s) - \mathbb{E}X(s)) \cdot \nu(X(s)) dL(s). \end{aligned}$$

Due to Assumption 5.2, we have

$$(X(s) - \mathbb{E}X(s)) \cdot \nu(X(s)) \leq 0.$$

Also, note that $\mathbb{E}((X(s) - \mathbb{E}X(s)) \cdot (\mathbb{E}X(s) - \bar{X}(s))) = 0$. Consequently, we get

$$\begin{aligned} \text{Var}(t) &:= \mathbb{E}|X(t) - \mathbb{E}X(t)|^2 \leq \mathbb{E}|X_0 - \mathbb{E}(X_0)|^2 - 2 \int_0^t \beta \mathbb{E}|X(s) - \mathbb{E}X(s)|^2 ds \\ &\quad + \int_0^t \sigma^2 \mathbb{E}|X(s) - \bar{X}(s)|^2 ds. \end{aligned}$$

We have

$$\mathbb{E}|X(s) - \bar{X}(s)|^2 = \mathbb{E}|X(s) - \mathbb{E}X(s)|^2 + |\mathbb{E}X(s) - \bar{X}(s)|^2 \quad (5.18)$$

and

$$\begin{aligned} |\mathbb{E}X(s) - \bar{X}(s)|^2 &= \left| \mathbb{E}X(s) - \frac{\mathbb{E}X(s)e^{-\alpha f(X(s))}}{\mathbb{E}e^{-\alpha f(X(s))}} \right|^2 \\ &= \left| \mathbb{E} \left((\mathbb{E}X(s) - X(s)) \frac{e^{-\alpha f(X(s))}}{\mathbb{E}e^{-\alpha f(X(s))}} \right) \right|^2 \\ &\leq e^{2\alpha f_{\text{osc}}} \mathbb{E}|X(s) - \mathbb{E}X(s)|^2. \end{aligned} \quad (5.19)$$

Therefore,

$$\frac{d}{dt} \text{Var}(t) \leq (-2\beta + \sigma^2(1 + e^{2\alpha f_{\text{osc}}})) \text{Var}(t) \leq (-2\beta + \sigma^2(1 + e^{2\alpha f_{\text{osc}}})) \text{Var}(t), \quad (5.20)$$

which implies

$$\text{Var}(t) \leq \text{Var}(0)e^{-\eta_0 t}. \quad (5.21)$$

This also means, due to (5.18) and (5.19), there exist positive constants c_1 and c_2 independent of t such that

$$\mathbb{E}|X(t) - \bar{X}(t)|^2 \leq c_1 e^{-\eta_0 t}, \quad (5.22)$$

$$|\mathbb{E}X(t) - \bar{X}(t)|^2 \leq c_2 e^{-\eta_0 t}. \quad (5.23)$$

Let us fix a constant $q \in G$. Then, again using Ito's formula, we have

$$\begin{aligned} d|X(t) - q|^2 &= -2\beta((X(t) - q) \cdot (X(t) - \bar{X}(t)))dt + \sigma^2|X(t) - \bar{X}(t)|^2 dt \\ &\quad + 2\sigma((X(t) - q) \cdot \text{Diag}(X(t) - \bar{X}(t))dW(t)) \\ &\quad + 2((X(t) - q) \cdot \nu(X(t)))dL(t). \end{aligned}$$

Using Tanaka's trick (thanks to Assumption 5.2) and taking expectation on both sides, we have

$$\begin{aligned} d\mathbb{E}|X(t) - q|^2 &\leq -2\beta\mathbb{E}((X(t) - q) \cdot (X(t) - \bar{X}(t)))dt + \sigma^2\mathbb{E}|X(t) - \bar{X}(t)|^2 dt \\ &\leq -2\beta\mathbb{E}((X(t) - q) \cdot (X(t) - \bar{X}(t)))dt + \sigma^2 c_1 e^{-\eta_0 t} dt, \end{aligned}$$

where we have used (5.22) in the last inequality. Splitting the term $((X(t) - q) \cdot (X(t) - \bar{X}(t)))$, we get

$$\begin{aligned} \frac{d}{dt} \mathbb{E}|X(t) - q|^2 &\leq -2\beta\mathbb{E}((X(t) - q) \cdot (X(t) - \bar{X}(t))) + \sigma^2 c_1 e^{-\eta_0 t} \\ &= -2\beta\mathbb{E}|X(t) - q|^2 + 2\beta((\mathbb{E}X(t) - q) \cdot (\bar{X}(t) - q)) + \sigma^2 c_1 e^{-\eta_0 t}. \end{aligned}$$

Rewriting $(\mathbb{E}X(t) - q) \cdot (\bar{X}(t) - q) = |\mathbb{E}X(t) - q|^2 + (\mathbb{E}X(t) - q) \cdot (\bar{X}(t) - \mathbb{E}X(t))$ gives

$$\begin{aligned} \frac{d}{dt} \mathbb{E}|X(t) - q|^2 &\leq -2\beta\mathbb{E}|X(t) - q|^2 + 2\beta\mathbb{E}|X(t) - q|^2 \\ &\quad + 2\beta(\mathbb{E}X(t) - q) \cdot (\bar{X}(t) - \mathbb{E}X(t)) + \sigma^2 c_1 e^{-\eta_0 t}. \end{aligned}$$

Due to Jensen's inequality, we get $|\mathbb{E}X(t) - q|^2 \leq \mathbb{E}|X(t) - q|^2$ which provides the following differential inequality:

$$\begin{aligned} \frac{d}{dt} \mathbb{E}|X(t) - q|^2 &\leq 2\beta(\mathbb{E}X(t) - q) \cdot (\bar{X}(t) - \mathbb{E}X(t)) + \sigma^2 c_1 e^{-\eta_0 t} \\ &\leq 2\beta\sqrt{c_2} |\mathbb{E}X(t) - q| e^{-\eta_0 t/2} + \sigma^2 c_1 e^{-\eta_0 t}. \end{aligned}$$

Note that $|\mathbb{E}X(t) - q|$ is bounded uniformly in t due to boundedness of the domain G . Therefore, we can say that there exists a constant $c_3 > 0$ such that

$$\frac{d}{dt} \mathbb{E}|X(t) - q|^2 \leq c_3 e^{-\eta_0 t/2}, \quad (5.24)$$

which together with (5.21) implies that there exists an $x^* \in \bar{G}$ such that $\mathbb{E}X(t)$ is converging to x^* as $t \rightarrow \infty$. Here, x^* belongs to \bar{G} due to convexity of G .

Using Markov's inequality, we get

$$\mathbb{P}(|X(t) - \mathbb{E}X(t)| \geq e^{-\eta_0 t/4}) \leq \frac{\mathbb{V}\text{ar}(t)}{e^{-\eta_0 t/2}} \leq C e^{-\eta_0 t/2},$$

where C is a positive constant independent of t . Then, using the Borel–Cantelli lemma, $|X(t) - \mathbb{E}X(t)| \rightarrow 0$ as $t \rightarrow \infty$ a.s., and hence $X(t) \rightarrow x^*$ a.s. Consequently, applying the bounded convergence theorem, we arrive at $\mathbb{E}e^{-\alpha f(X(t))} \rightarrow e^{-\alpha f(x^*)}$ as $t \rightarrow \infty$. Therefore, we can say: for all $\epsilon > 0$ there exists a $T^* > 0$ such that

$$|\mathbb{E}e^{-\alpha f(X(t))} - e^{-\alpha f(x^*)}| \leq \epsilon \quad (5.25)$$

for all $t \geq T^*$. Since the probability distribution of $X(T^*)$ is compactly supported, using the Laplace principle we obtain

$$-\frac{1}{\alpha} \log(\mathbb{E}e^{-\alpha f(X(T^*))}) \leq f_{\min} + \Gamma_1(\alpha), \quad (5.26)$$

where $\Gamma_1(\alpha) \rightarrow 0$ as $\alpha \rightarrow \infty$. And, from (5.25), we have

$$\mathbb{E}e^{-\alpha f(X(T^*))} \leq \epsilon + e^{-\alpha f(x^*)},$$

which implies

$$\begin{aligned} \log \mathbb{E}e^{-\alpha f(X(T^*))} &\leq \log(\epsilon + e^{-\alpha f(x^*)}), \\ -\frac{1}{\alpha} \log \mathbb{E}e^{-\alpha f(X(T^*))} &\geq -\frac{1}{\alpha} \log(\epsilon + e^{-\alpha f(x^*)}). \end{aligned} \quad (5.27)$$

Using (5.26) and (5.27), we obtain

$$-\frac{1}{\alpha} \log(\epsilon + e^{-\alpha f(x^*)}) \leq f_{\min} + \Gamma_1(\alpha). \quad (5.28)$$

From the mean value theorem, we have

$$\log(\epsilon + e^{-\alpha f(x^*)}) = -\alpha f(x^*) + \frac{\epsilon}{\gamma\epsilon + e^{-\alpha f(x^*)}}, \quad (5.29)$$

for some $\gamma \in (0, 1)$. Therefore,

$$f(x^*) \leq f_{\min} + \Gamma_1(\alpha) + \frac{\epsilon}{\alpha} \frac{1}{\gamma\epsilon + e^{-\alpha f(x^*)}}. \quad \square$$

Theorem 5.3. *Let Assumptions 2.1 and 5.2 hold. Let*

$$\eta_1 := -2\beta + 3\lambda(0) + \sigma^2(1 + e^{2\alpha f_{osc}})$$

be strictly greater than a positive constant K_1 . If $0 \leq \lambda(t) \leq K_2 \exp(-\eta_2 t)$ for some $K_2 > 0$ and $\eta_2 > \eta_1$, then there exists an $x^ \in \bar{G}$ such that $X(t) \rightarrow x^*$ as $t \rightarrow \infty$ and*

$$f(x^*) \leq f_{\min} + \Gamma(\alpha),$$

where $\Gamma(\alpha) \rightarrow 0$ as $\alpha \rightarrow \infty$.

Proof. Using Ito's formula, we have

$$\begin{aligned} & |X(t) - \mathbb{E}X(t)|^2 \\ &= |X(0) - \mathbb{E}X(0)|^2 - 2 \int_0^t \beta(X(s) - \mathbb{E}X(s)) \cdot (X(s) - \bar{X}(s)) ds \\ &\quad + 2 \int_0^t \lambda(s) \int_G ((X(s) - \mathbb{E}X(s)) \cdot (X(s) - y)) \\ &\quad \times \exp\left(-\frac{1}{2}|X(s) - y|^2\right) \mathcal{L}_{X(s)}(dy) ds \\ &\quad + 2 \int_0^t \sigma((X(s) - \mathbb{E}X(s)) \cdot \text{Diag}(X(s) - \bar{X}(s))) dW(s) \\ &\quad + \int_0^t \sigma^2 |X(s) - \bar{X}(s)|^2 ds + 2 \int_0^t ((X(s) - \mathbb{E}X(s)) \cdot \nu(X(s))) dL(s). \end{aligned}$$

The objective here is to deal with the repelling term. In that pursuit, we apply Young's inequality to get

$$\begin{aligned} & \mathbb{E} \int_G ((X(s) - \mathbb{E}X(s)) \cdot (X(s) - y)) \exp\left(-\frac{1}{2}|X(s) - y|^2\right) \mathcal{L}_{X(s)}(dy) \\ & \leq \frac{1}{2} \mathbb{E} |X(s) - \mathbb{E}X(s)|^2 \\ & \quad + \frac{1}{2} \mathbb{E} \int_G |X(s) - y|^2 \exp\left(-\frac{1}{2}|X(s) - y|^2\right) \mathcal{L}_{X(s)}(dy) \\ & \leq \frac{1}{2} \mathbb{E} |X(s) - \mathbb{E}X(s)|^2 + \frac{1}{2} \mathbb{E} \int_G |X(s) - y|^2 \mathcal{L}_{X(s)}(dy) \\ & \leq \frac{3}{2} \mathbb{E} |X(s) - \mathbb{E}X(s)|^2, \end{aligned} \tag{5.30}$$

since $\mathbb{E} \int_{\mathbb{R}^d} |X(s) - y|^2 \mathcal{L}_{X(s)}(dy) = 2\mathbb{E} |X(s) - \mathbb{E}X(s)|^2$.

Exploiting similar arguments as the ones used to get (5.20) and using the inequality obtained in (5.30), we ascertain

$$\frac{d}{dt} \mathbb{V}\text{ar}(t) \leq (-2\beta + 3\lambda(0) + \sigma^2(1 + e^{2\alpha f_{\text{osc}}})) \mathbb{V}\text{ar}(t).$$

With an appropriate choice of β , σ and of decreasing $\lambda(t)$, we have

$$\frac{d}{dt} \mathbb{V}\text{ar}(t) \leq c_4 e^{-\eta_1 t},$$

where c_4 and η_1 are independent of t .

Let us again fix a constant $q \in G$. Applying Ito's formula gives

$$\begin{aligned} d|X(t) - q|^2 &= -2\beta((X(t) - q) \cdot (X(t) - \bar{X}(t)))dt + \sigma^2|X(t) - \bar{X}(t)|^2 dt \\ &\quad + 2\lambda(t) \int_G ((X(t) - q) \cdot (X(t) - y)) \exp\left(-\frac{1}{2}|X(t) - y|^2\right) \mathcal{L}_{X(t)}(dy) \\ &\quad + 2\sigma((X(t) - q) \cdot \text{Diag}(X(t) - \bar{X}(t)))dW(t) \\ &\quad + 2((X(t) - q) \cdot \nu(X(t)))dL(t). \end{aligned}$$

Using Young's inequality, we have

$$\begin{aligned} &\int_G ((X(t) - q) \cdot (X(t) - y)) \exp\left(-\frac{1}{2}|X(t) - y|^2\right) \mathcal{L}_{X(t)}(dy) \\ &= \frac{1}{2}|X(t) - q|^2 \int_G \exp\left(-\frac{1}{2}|X(t) - y|^2\right) \mathcal{L}_{X(t)}(dy) \\ &\quad + \frac{1}{2} \int_G |X(t) - y|^2 \exp\left(-\frac{1}{2}|X(t) - y|^2\right) \mathcal{L}_{X(t)}(dy) \\ &\leq \frac{1}{2}|X(t) - q|^2 + \int_G \frac{1}{2}|X(t) - y|^2 \mathcal{L}_{X(t)}(dy). \end{aligned}$$

Using analogous arguments employed to obtain (5.24), we get

$$\begin{aligned} \frac{d}{dt} \mathbb{E}|X(t) - q|^2 &\leq c_5 e^{-\eta_1 t/2} + \lambda(t) \mathbb{E}|X(t) - q|^2 + \lambda(t) \mathbb{E} \int_G |X(t) - y|^2 \mathcal{L}_{X(t)}(dy) \\ &\leq c_5 e^{-\eta_1 t/2} + \lambda(t) \mathbb{E}|X(t) - q|^2 + 2\lambda(t) c_4 e^{-\eta_1 t}, \end{aligned} \quad (5.31)$$

where $c_5 > 0$ is a constant independent of t . Note that $\mathbb{E}|X(t) - q|^2$ is bounded uniformly in t . Since the function $\lambda(t)$ tends to zero faster than $e^{-\eta_1 t}$ as $t \rightarrow \infty$, we get that $\mathbb{E}|X(t) - q|^2$ converges to a constant as $t \rightarrow \infty$. Therefore, there is an $x^* \in \bar{G}$ such that $\mathbb{E}X(t) \rightarrow x^*$ as $t \rightarrow \infty$. The rest of the arguments to complete the proof are the same as used in the previous theorem. \square

6. Numerical Tests

In this section, we first (Sec. 6.1) consider discrete approximations of the interacting particle systems and then perform several numerical experiments to demonstrate effectiveness of the CBO models described in Sec. 2.2 for constrained optimization.

Since these CBO algorithms are probabilistic in nature and convergence is guaranteed only asymptotically (in N , α and t), we report the success rate of each experiment for a finite N , α and t . Each experiment is run 10^3 times (except the experiment in Sec. 6.3, which is only run 100 times), and the success rate is simply the proportion of experiments which successfully find the true global minimizer. We declare an experiment successful if the final consensus is within $\varepsilon > 0$ of the location of the true minimizer. For each experiment, we use the threshold $\varepsilon = 0.1$ unless otherwise specified.

We note briefly that there are several parameters/controls for the CBO algorithms: (i) the inverse temperature, α ; (ii) the number of particles, N ; (iii) strength of the drift and diffusion coefficients, β and σ , respectively; (iv) the integration time, t ; and (v) the step size, h , of a numerical scheme approximating the particle system. We do not attempt to propose a systematic way of choosing these parameters, but instead opt for sensible and practically effective choices in the following experiments. In general, α and N should be chosen as large as possible. For α , we run the risk of numerical instability if it is chosen too large. For N , the computational cost of the algorithm is at least $\mathcal{O}(N)$ (and $\mathcal{O}(N^2)$ in the case of the repelling CBO model from Sec. 2.2.2), so there is a trade-off that must be balanced. As such, in Secs. 6.2–6.5, we explore success rates for varying values of N . Similar comments can be made about the number of steps of the numerical scheme.

The strength of drift, β , and diffusion σ , coefficients can also depend on time. We experiment with both of them being constant in Secs. 6.2, 6.3, and 6.5 but also linearly increasing (β) and exponentially decreasing (σ) functions in Secs. 6.4 and 6.6. In all the experiments for the penalty scheme (6.1) given below the optimal choice of the penalty $\epsilon = h$ was used.

The presented experiments are implemented in Python, using the PyTorch library, and the code is available at <https://github.com/piers-hinds/RMVSDE-numerics>.

6.1. Approximation of the interacting particle system

To implement optimization or sampling methods based on mean-field SDEs, we need to be able to simulate the interacting particle system (2.3). Consider a uniform discretization of the time-interval $[0, T]$, for a fixed $T > 0$, such that $t_{k+1} - t_k = h$, $k = 0, \dots, K - 1$ and $T = Kh$.

In the case of CBO models like the ones from Sec. 2.2 we need numerical methods for (2.3) converging in the almost sure sense. There are two types of mean-square/almost sure methods for reflected SDEs in the literature: penalty and projection (see e.g. Refs. 54 and 61). Denote by $\Pi(x)$ the projection of x on ∂G if

$x \notin \bar{G}$ else $\Pi(x) = x$. Introduce the function (penalty) $\pi(x) = (x - \Pi(x))$, which is half of the gradient of square of distance function of x from ∂G . Let $Y_k^{i,N}$ be an approximation of (2.3). The penalty and projection schemes for reflected SDEs adapted to the interacting particle system (2.3) take the form

(i) Penalty scheme:

$$Y_{k+1}^{i,N} = Y_k^{i,N} + b(t_k, Y_k^{i,N}, \hat{\mu}_{\mathbf{Y}_k^N})h + \sigma(t_k, Y_k^{i,N}, \hat{\mu}_{\mathbf{Y}_k^N})\Delta W^i(t_k) - \frac{h}{\epsilon}\pi(Y_k^{i,N}), \quad i = 1, \dots, N, \quad (6.1)$$

where $\Delta W^i(t_k) = W^i(t_{k+1}) - W^i(t_k)$ are the Wiener increments. The optimal choice of the penalty strength ϵ is h (see Ref. 61).

(ii) Projection scheme:

$$\begin{aligned} \bar{Y}_{k+1}^{i,N} &= Y_k^{i,N} + b(t_k, Y_k^{i,N}, \hat{\mu}_{\mathbf{Y}_k^N})h + \sigma(t_k, Y_k^{i,N}, \hat{\mu}_{\mathbf{Y}_k^N})\Delta W^i(t_k), \\ Y_{k+1}^{i,N} &= \Pi(\bar{Y}_{k+1}^{i,N}), \quad i = 1, \dots, N. \end{aligned} \quad (6.2)$$

There are rather limited numerical analysis results for mean-square convergence of these two methods. In the case of convex polyhedra, the mean-square order of convergence of both methods is $1/2$ up to a logarithmic correction, and in the case of smooth convex domains, mean-square order of $1/4$ has been proved (see, e.g. Refs. 54 and 61). Like in Ref. 38 one can potentially show that mean-square convergence of these methods is uniform in number of particles N , considering this aspect is beyond the scope of this paper.

For sampling methods, it is sufficient to use weak-sense schemes for approximating (2.3). Weak methods for reflected SDEs are available in Refs. 51, 11, 41 and 52.

6.2. Ackley function

We begin with the Ackley function, which is a widely used benchmark function for global optimization problems.² The function is defined as

$$f(x, y) = -20 \exp \left(-0.2 \sqrt{\frac{1}{2}(x^2 + y^2)} \right) - \exp \left(\frac{1}{2}(\cos(2\pi x) + \cos(2\pi y)) \right) + 20 + e. \quad (6.3)$$

We translate the function so that the global minimum is located at $(2, 2)$ instead of $(0, 0)$. The feasible region is the closed ball of radius 3 centered at the origin:

$$\bar{G} = \{(x, y) : x^2 + y^2 \leq 9\}. \quad (6.4)$$

The function with constraints is illustrated in Fig. 2. We choose drift $\beta = 1$ and diffusion $\sigma = 4$, time $t = 1$, $\alpha = 10^4$. The initial position of the particles is sampled from a uniform distribution on the feasible region. Both the penalty scheme

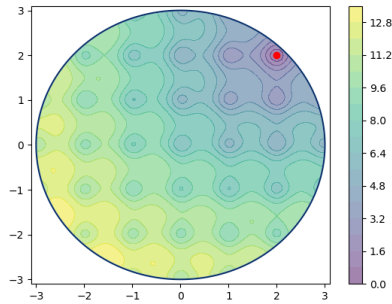


Fig. 2. Translated Ackley function with minimum at $(2, 2)$ constrained to a closed ball of radius 3.

Table 1. Translated Ackley function. Comparison of success rates for the penalty and projection schemes.

(a) Penalty scheme					(b) Projection scheme				
$1/h$	N				$1/h$	N			
	10	20	50	100		10	20	50	100
5	0.055	0.137	0.416	0.717	5	0.137	0.370	0.809	0.979
10	0.256	0.605	0.966	1.000	10	0.550	0.926	1.000	1.000
20	0.762	0.986	1.000	1.000	20	0.883	0.997	1.000	1.000
50	0.725	0.973	1.000	1.000	50	0.730	0.978	1.000	1.000
100	0.317	0.728	0.993	1.000	100	0.307	0.717	0.993	1.000

(6.1) and the projection scheme (6.2) are tested and the success rates for various numbers of particles, N , and number of time steps, $1/h$ (in other words, choice of h with the fixed $t = 1$), are reported in Table 1. We observe that both penalty and projection schemes converge reliably to the global minimizer as N and the number of steps increases. Both approaches exhibit broadly similar performance, achieving near 100% success for modestly large N and sufficiently many steps. The projection method performs slightly better, which could be due to the fact that when the consensus is computed, all particles are guaranteed to lie within the feasible region.

6.3. Non-convex function with heart-shaped constraint

We now consider a non-convex function from Ref. 67 defined as

$$f(x, y) = -[\cos((x - 0.1)y)]^2 - x \sin(3x + y) \tag{6.5}$$

constrained to a heart-shaped region given by the inequality:

$$x^2 + y^2 \leq \left[2 \cos(t) - \frac{1}{2} \cos(2t) - \frac{1}{4} \cos(3t) - \frac{1}{8} \cos(4t) \right]^2 + 4 \sin^2(t), \tag{6.6}$$

where $t = \text{atan2}(x, y)$. The function and the feasible region are shown in Fig. 3. The level-set nature of the constraint means that we can project particles on the boundary of the domain in the following manner. First, if a particle lies outside the feasible region, the inward normal direction to the level set can be computed.

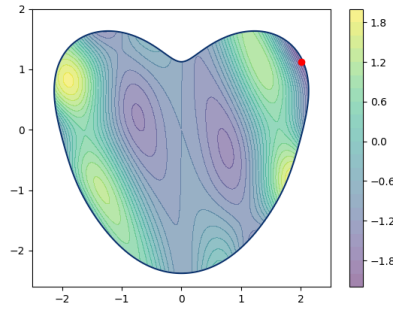


Fig. 3. Non-convex function with heart-shaped constraint.

Second, using this normal direction, we can solve — by Newton’s method — for the distance along this normal we need to translate the particle such that it will lie on the boundary. Note that the domain is non-convex.

Like before, we use drift $\beta = 1$, diffusion $\sigma = 4$ and $\alpha = 10^4$. Further, we use a fixed time step of $h = 1/20$. For the initial state of the particles, we sample uniformly in a ball of radius $5/2$ before projecting onto the feasible region. We report success rates using the projection scheme (6.2) for various values of N and number of time steps K in Table 2. The results in Table 2 indicate that the CBO method reliably finds the global minimizer despite the non-convex nature of the domain. The observed success rates generally increase with N and time (number of steps K), as would be expected.

6.4. High-dimensional Rastrigin function

We consider the Rastrigin function in various dimensions. It is defined as

$$f(x) = 10d + \sum_{i=1}^d (x_i^2 - 10 \cos(2\pi x_i)), \quad (6.7)$$

constrained to the closed ball of radius 5 centered at the origin: $\bar{G} = \{x \in \mathbb{R}^d : |x| \leq 5\}$. Instead of constant drift and diffusion coefficients, β and σ , we use $\beta(t) = 10t$, $\sigma(t) = 10e^{-t \log 10}$, so that the drift increases by an order of magnitude over the interval $[0, 1]$, while σ decreases by an order of magnitude. We take $\alpha = 10^4$ and a

Table 2. Success rates of the CBO method on the non-convex function with heart-shaped constraint.

K	N			
	10	20	50	100
5	0.29	0.54	0.90	0.95
10	0.46	0.69	0.88	0.99
20	0.54	0.81	0.95	1.00
50	0.59	0.78	0.98	0.99
100	0.57	0.81	0.97	1.00

Table 3. Comparison of success rates for the Rastrigin function in various dimensions for number of iterations $K = 200, 500$, and 1000 .

(a) $K = 200$

d	N			
	10	20	50	100
5	0.194	0.472	0.834	0.982
20	0.080	0.203	0.549	0.800
100	0.031	0.086	0.237	0.417
500	0.030	0.047	0.075	0.141

(b) $K = 500$

d	N			
	10	20	50	100
5	0.251	0.533	0.899	0.993
20	0.159	0.459	0.841	0.948
100	0.095	0.275	0.750	0.950
500	0.059	0.174	0.492	0.819

(c) $K = 1000$

d	N			
	10	20	50	100
5	0.263	0.523	0.903	0.991
20	0.167	0.456	0.825	0.951
100	0.077	0.321	0.779	0.958
500	0.060	0.181	0.506	0.845

step size of $h = 1/500$ is used. The initial position of the particles is sampled from a uniform distribution on the feasible region.

Success rates using the projection scheme (6.2) are given in Table 3 for various values of dimension, d , and number of particles, N . We also consider the cases where we have the number of iterations $K = 200, 500$, and 1000 . The results in Table 3 highlight the scalability of the algorithm to higher-dimensional settings. While success rates decline with increasing dimensionality, they remain high for modestly large N . We also see an increase in success rates as K increases, particularly between $K = 200$ and $K = 500$.

6.5. Testing repelling CBO on Rosenbrock function

Let us now consider the Rosenbrock function in two dimensions, defined as

$$f(x,y) = (1-x)^2 + 100(y-x^2)^2.$$
 (6.8)

In addition we consider the feasible region

$$\bar{G} = \{(x,y) \in \mathbb{R}^2 : x^2 + y^2 \leq 2\},$$
 (6.9)

such that the minimizer of f , $(1,1)$, lies on the boundary of G . The feasible region and the Rosenbrock function are displayed in Fig. 4.

In this experiment, we compare the CBO method from Sec. 2.2.1 with the repelling CBO method from Sec. 2.2.2. In Table 4, success rates for both methods are shown for different values of N and K . We use the projection scheme (6.2) with a fixed step size of $h = 1/20$ for each experiment, as well as a drift parameter $\beta = 1$ and diffusion parameter $\sigma = 4$ and $\alpha = 10^4$. The initial position of the particles is sampled from a uniform distribution on the feasible region. The comparison in Table 4 illustrates the better performance of the repelling CBO method over the standard CBO method, especially for smaller N and K . The repelling method's

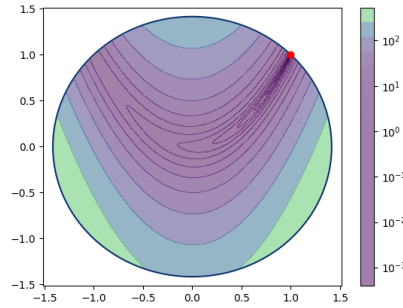


Fig. 4. Rosenbrock function constrained to a closed ball of radius $\sqrt{2}$.

Table 4. Constrained Rosenbrock function. Comparison of success rates between standard and repelling constrained CBO.

(a) Success rates for the standard CBO					(b) Success rates for the repelling CBO				
<i>K</i>	<i>N</i>				<i>K</i>	<i>N</i>			
	10	20	50	100		10	20	50	100
5	0.075	0.106	0.192	0.332	5	0.182	0.340	0.665	0.863
10	0.084	0.135	0.281	0.525	10	0.214	0.384	0.669	0.834
20	0.094	0.169	0.422	0.766	20	0.234	0.433	0.765	0.915
50	0.121	0.249	0.702	0.982	50	0.263	0.538	0.929	0.999
100	0.133	0.315	0.892	0.999	100	0.287	0.595	0.979	1.000

ability to aid with exploration seems particularly relevant in this example, since it allows particles to continue exploring even when they are in a good location relative to other particles.

We remark that although the repelling method outperforms the standard CBO method, this is at the cost of additional computational complexity. Since pairwise interactions are computed, the repelling method is of $\mathcal{O}(N^2)$ complexity. However, it still requires only N objective function evaluations per iteration. Thus, we can achieve better performance without any additional function evaluations which may be relevant when, for example, the objective function is expensive to evaluate. There are ways to overcome the $\mathcal{O}(N^2)$ complexity via locality sensitive hashing or efficient nearest neighbor search, see Ref. 27 for example.

6.6. Inverse problem

In this section, we test the CBO model from Sec. 2.2.1 on an inverse problem. Consider the Cauchy problem for the parabolic partial integral differential equation (PIDE):

$$\begin{aligned} \frac{\partial u}{\partial t} + \frac{1}{2}\sigma^2 x^2 \frac{\partial^2 u}{\partial x^2} - bx \frac{\partial u}{\partial x} \\ + \frac{1}{\sqrt{2\pi\gamma^2}} \int_{\mathbb{R}} [u(t, xe^y) - u(t, x)] \exp\left(-\frac{(y-m)^2}{2\gamma^2}\right) dy = 0, \end{aligned} \tag{6.10}$$

with the terminal condition

$$u(T, x) = \max\{x - 1, 0\} \quad (6.11)$$

and $b := e^{m + \frac{1}{2}\gamma^2} - 1$.

The inverse problem is formulated within Tikhonov's regularization setup as follows. Given noisy observations $\hat{u}_{i,j}$ of the solution $u(t_i, x_j)$ to the PIDE problem (6.10) at some t_i, x_j , we aim to find estimates $\hat{\theta} := (\hat{\sigma}, \hat{m}, \hat{\gamma})$ of the parameters $\theta = (\sigma, m, \gamma)$ with the constraints $\hat{\sigma} \in [0, 1]$, $\hat{m} \in [-1, 1]$, and $\hat{\gamma} \in [0, 1]$. To achieve this aim, we construct the loss function

$$\text{Loss}(\theta) = \sum_{i=1}^{10} \sum_{j=1}^5 |u(t_i, x_j; \theta) - \hat{u}_{i,j}|^2 + \lambda |\theta|_2, \quad (6.12)$$

where $\lambda > 0$ is a small regularization parameter (we use $\lambda = 10^{-5}$ in the experiments). The data are synthetically generated using the following representation for the forward map⁵⁰:

$$u(t, x; \theta) = \sum_{j=0}^{\infty} \frac{(\tau)^j}{j!} e^{-\tau} \left\{ x e^{-b\tau + j(m + \gamma^2/2)} \Phi\left(\frac{\ln(x) + (\frac{\sigma^2}{2} - b)\tau + j(m + \gamma^2)}{\sqrt{\sigma^2\tau + j\gamma^2}}\right) - \Phi\left(\frac{\ln(x) + (-\frac{\sigma^2}{2} - b)\tau + jm}{\sqrt{\sigma^2\tau + j\gamma^2}}\right) \right\}, \quad \tau = T - t, \quad (6.13)$$

followed by adding a small amount of relative (observational) noise

$$\hat{u}_{ij} = u(t_i, x_j; \theta) + \epsilon_{ij}, \quad \epsilon_{ij} \sim \mathcal{N}(0, 10^{-3}u(t_i, x_j; \theta)). \quad (6.14)$$

Here $\Phi(\cdot)$ is the cdf for the standard normal distribution. We approximate the infinite series in (6.13) by summing the first 20 terms or truncating when the magnitude of the summand falls below 10^{-14} , whichever occurs first. Note that when the forward map is not available in an analytical form, linear PIDE problems can be solved using the Monte Carlo technique together with approximating the corresponding stochastic characteristics by a suitable numerical scheme (see e.g. Ref. 21 and references therein).

For the experiments we take $T = 3$ and use the uniformly spaced grid $t_i = 0.3(i - 1)$, $i = 1, \dots, 10$, and $x_j = 0.8 + 0.1(j - 1)$, $j = 1, \dots, 5$. As the ground truth, we chose $\sigma = 0.1$, $m = -0.2$, $\gamma = 0.3$, which are the true values to be recovered. We use $N = 400$ particles and the projection scheme (6.2) with step-size $h = 0.01$ together with the drift and diffusion coefficients described in Sec. 6.4. The initial distribution for the particles is taken to be uniform on $[0, 1] \times [-1, 1] \times [0, 1]$. We run the projection scheme for $K = 100$ steps. Additionally, we use the tolerance $\varepsilon = 0.01$ to determine if an experiment is successful. Using a value of $\alpha = 10^{14}$, we obtain a success rate of 0.99 on 100 experiments. We note that in this case, a value of $\alpha = 10^4$ is not sufficient and results in a success rate of 0.07.

In Fig. 5, we include the histograms for each parameter in the final consensus of each experiment. We see that each estimated parameter is distributed reasonably

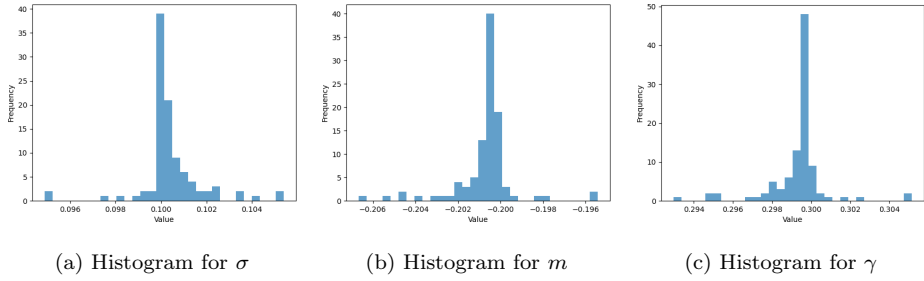


Fig. 5. The inverse problem. Histograms of recovered parameters across the 100 experiments.


tightly around the true parameter value. In a future work it is of interest to test the constrained CBO models from Sec. 2.2 on more complex inverse problems.


Acknowledgments


The authors are grateful to Professor Alain-Sol Sznitman and Dr Axel Ringh for useful discussions. AS and MVT were supported by the Engineering and Physical Sciences Research Council (grant number EP/X022617/1). AS was also supported by the Wallenberg AI, Autonomous Systems and Software Program (WASP) funded by the Knut and Alice Wallenberg Foundation. AS and MVT thank the Isaac Newton Institute for Mathematical Sciences (Cambridge, UK), funded by EPSRC grant EP/Z000580/1, for support and hospitality during the programme “Stochastic systems for anomalous diffusion”, where a part of work on this paper was undertaken.

For the purpose of open access, the authors applied a Creative Commons Attribution (CC-BY) license to any Author Accepted Manuscript version arising.

ORCID

Piers D. Hinds  <https://orcid.org/0009-0003-5822-826X>

Akash Sharma  <https://orcid.org/0009-0003-3102-4814>

Michael V. Tretyakov  <https://orcid.org/0000-0002-7929-9046>

References

1. D. Adams, G. dos Reis, R. Ravaille, W. Salkeld and J. Tugaut, Large deviations and exit-times for reflected McKean–Vlasov equations with self-stabilising terms and superlinear drifts, *Stoch. Proc. Appl.* **146** (2022) 264–310.
2. T. Back, *Evolutionary Algorithms in Theory and Practice: Evolution Strategies, Evolutionary Programming, Genetic Algorithms* (Oxford Univ. Press, 1996).
3. H.-O. Bae, S.-Y. Ha, M. Kang, H. Lim, C. Min and J. Yoo, A constrained consensus based optimization algorithm and its application to finance, *Appl. Math. Comput.* **416** (2022) 126726.
4. J. Beddrich, E. Chenchene, M. Fornasier, H. Huang and B. Wohlmuth, Constrained consensus-based optimization and numerical heuristics for the few particle regime, preprint (2024), arXiv: 2410.10361.

5. N. Bellomo, D. Burini, G. Dosi, L. Gibelli, D. Knopoff, N. Outada, P. Terna and M. E. Virgillito, What is life? A perspective of the mathematical kinetic theory of active particles, *Math. Models Methods Appl. Sci.* **31** (2021) 1821–1866.
6. N. Bellomo, J. Liao, A. Quaini, L. Russo and C. Siettos, Human behavioral crowds review, critical analysis and research perspectives, *Math. Models Methods Appl. Sci.* **33** (2023) 1611–1659.
7. V. I. Bogachev and A. V. Kolesnikov, The Monge–Kantorovich problem: Achievements, connections, and perspectives, *Russ. Math. Surv.* **67** (2012) 785–890.
8. F. Bolley, Separability and completeness for the Wasserstein distance, in *Séminaire de Probabilités XLI*, eds. C. Donati-Martin, M. Émery, A. Rouault and C. Stricker, Lecture Notes in Mathematics (Springer, 2008), pp. 371–377.
9. J. Bolte, L. Miclo and S. Villeneuve, Swarm gradient dynamics for global optimization: The mean-field limit case, *Math. Program.* **205** (2024) 661–701.
10. G. Borghi, M. Herty and L. Pareschi, Constrained consensus-based optimization, *SIAM J. Optim.* **33** (2023) 211–236.
11. M. Bossy, E. Gobet and D. Talay, A symmetrized Euler scheme for an efficient approximation of reflected diffusions, *J. Appl. Probab.* **41** (2004) 877–889.
12. B. Bouchard, Optimal reflection of diffusions and barrier options pricing under constraints, *SIAM J. Control Optim.* **47** (2008) 1785–1813.
13. J. A. Carrillo, Y.-P. Choi, C. Totzeck and O. Tse, An analytical framework for consensus-based global optimization method, *Math. Models Methods Appl. Sci.* **28** (2018) 1037–1066.
14. J. A. Carrillo, A. Clini and S. Solem, The mean field limit of stochastic differential equation systems modeling grid cells, *SIAM J. Math. Anal.* **55** (2023) 3602–3634.
15. J. A. Carrillo, F. Hoffmann, A. M. Stuart and U. Vaes, Consensus-based sampling, *Stud. Appl. Math.* **148** (2022) 1069–1140.
16. J. A. Carrillo, S. Jin, L. Li and Y. Zhu, A consensus-based global optimization method for high dimensional machine learning problems, *ESAIM. COCV* **27** (2021) S5.
17. J. A. Carrillo, R. J. McCann and C. Villani, Contractions in the 2-Wasserstein length space and thermalization of granular media, *Arch. Ration. Mech. Anal.* **179** (2006) 217–263.
18. J. A. Carrillo, C. Totzeck and U. Vaes, Consensus-based optimization and ensemble Kalman inversion for global optimization problems with constraints, in *Modeling and Simulation for Collective Dynamics* (World Scientific, 2023), pp. 195–230.
19. N. K. Chada, C. Schillings and S. Weissmann, On the incorporation of box-constraints for ensemble Kalman inversion, *Found. Data Sci.* **1** (2019) 433–456.
20. M. F. Chen and S.-F. Li, Coupling methods for multidimensional diffusion processes, *Ann. Probab.* **17** (1989) 151–177.
21. G. Deligiannidis, S. Maurer and M. V. Tretyakov, Random walk algorithm for the Dirichlet problem for parabolic integro-differential equation, *BIT Numer. Math.* **61** (2021) 1223–1269.
22. Z. Ding, M. Guerra, Q. Li and E. Tadmor, Swarm-based gradient descent meets simulated annealing, preprint (2024), arXiv:2404.18015.
23. A. Eberle, Reflection couplings and contraction rates for diffusions, *Probab. Theory Related Fields* **166** (2016) 851–886.
24. R. C. Fetecau, H. Huang and W. Sun, Propagation of chaos for the Keller–Segel equation over bounded domains, *J. Diff. Equations* **266** (2019) 2142–2174.
25. N. Fournier and A. Guillin, On the rate of convergence in Wasserstein distance of the empirical measure, *Probab. Theory Related Fields* **162** (2015) 707–738.

26. M. Freidlin, *Functional Integration and Partial Differential Equations* (Princeton Univ. Press, 1985).
27. D. Frenkel and B. Smit, *Understanding Molecular Simulation: From Algorithms to Applications* (Elsevier, 2023).
28. A. Garbuno-Inigo, F. Hoffmann, W. Li and A. M. Stuart, Interacting Langevin diffusions: Gradient structure and ensemble Kalman sampler, *SIAM J. Appl. Dynam. Syst.* **19** (2020) 412–441.
29. A. Garbuno-Inigo, N. Nusken and S. Reich, Affine invariant interacting Langevin dynamics for Bayesian inference, *SIAM J. Appl. Dynam. Syst.* **19** (2020) 1633–1658.
30. E. Gobet, Euler schemes and half-space approximation for the simulation of diffusion in a domain, *ESAIM Probab. Stat.* **5** (2001) 261–297.
31. S.-Y. Ha, S. Jin and D. Kim, Convergence of a first-order consensus-based global optimization algorithm, *Math. Models Methods Appl. Sci.* **30** (2020) 2417–2444.
32. S.-Y. Ha and E. Tadmor, From particle to kinetic and hydrodynamic descriptions of flocking, *Kinetic Related Models* **1** (2008) 415–435.
33. M. Hanu and S. Weissmann, On the ensemble Kalman inversion under inequality constraints, *Inverse Probl.* **40** (2024) 095009.
34. R. Horst, P. M. Pardalos and N. Van Thoai, *Introduction to Global Optimization* (Springer, 2000).
35. K. Hu, Z. Ren, D. Šiška and L. Szpruch, Mean-field Langevin dynamics and energy landscape of neural networks, *Ann. Inst. H. Poincaré (B) Probab. Statist.* **57** (2021) 2043–2065.
36. M. A. Iglesias, K. Law and A. M. Stuart, Ensemble Kalman methods for inverse problems, *Inverse Probl.* **29** (2013) 045001.
37. N. Ikeda and S. Watanabe, *Stochastic Differential Equations and Diffusion Processes* (North-Holland, 1989).
38. D. Kalise, A. Sharma and M. V. Tretyakov, Consensus-based optimization via jump-diffusion stochastic differential equations, *Math. Models Methods Appl. Sci.* **33** (2023) 289–339.
39. J. Kennedy and R. Eberhart, Particle swarm optimization, in *Proc. ICNN'95 - Int. Conf. Neural Networks*, Vol. 4 (IEEE, 1995), pp. 1942–1948.
40. B. Leimkuhler, C. Matthews and J. Weare, Ensemble preconditioning for Markov chain Monte Carlo simulation, *Stat. Comput.* **28** (2018) 277–290.
41. B. Leimkuhler, A. Sharma and M. V. Tretyakov, Simplest random walk for approximating Robin boundary value problems and ergodic limits of reflected diffusions, *Ann. Appl. Probab.* **33** (2023) 1904–1960.
42. B. Leimkuhler, A. Sharma and M. V. Tretyakov, Numerical integrators for confined Langevin dynamics, preprint (2024), arXiv:2404.16584.
43. B. Leimkuhler, T. J. Vlaar, T. Pouchon and A. Storkey, Better training using weight-constrained stochastic dynamics, in *Proc. 38th Int. Conf. Machine Learning*, eds. M. Meila and T. Zhang, Proceedings of Machine Learning Research, Vol. 139 (PMLR, 2021), pp. 6200–6211.
44. D. Lepingle, Euler scheme for reflected stochastic differential equations, *Math. Comput. Simul.* **38** (1995) 119–126.
45. T. Lindvall and L. C. G. Rogers, Coupling of multidimensional diffusions by reflection, *Ann. Probab.* **14** (1986) 860–872.
46. P.-L. Lions and A.-S. Sznitman, Stochastic differential equations with reflecting boundary conditions, *Commun. Pure Appl. Math.* **37** (1984) 511–537.

47. Q. Liu and D. Wang, Stein variational gradient descent: A general purpose Bayesian inference algorithm, in *Proc. 30th Int. Conf. Neural Information Processing Systems* (Curran Associates Inc., 2016), pp. 2378–2386.
48. F. Malrieu, Convergence to equilibrium for granular media equations and their euler schemes, *Ann. Appl. Probab.* **13** (2003) 540–560.
49. S. Mei, A. Montanari and P.-M. Nguyen, A mean field view of the landscape of two-layer neural networks, *Proc. Nation. Acad. Sci.* **115** (2018) E7665–E7671.
50. R. C. Merton, Option pricing when underlying stock returns are discontinuous, *J. Finan. Econom.* **3** (1976) 125–144.
51. G. N. Milstein, Application of the numerical integration of stochastic equations for the solution of boundary value problems with Neumann boundary conditions, *Theor. Prob. Appl.* **41** (1997) 170–177.
52. G. N. Milstein and M. V. Tretyakov, *Stochastic Numerics for Mathematical Physics* (Springer, 2021).
53. J. Nocedal and S. Wright, *Numerical Optimization* (Springer, 2006).
54. R. Pettersson, Approximations for stochastic differential equations with reflecting convex boundaries, *Stoch. Proc. Appl.* **59** (1995) 295–308.
55. A. Pilipenko, *An Introduction to Stochastic Differential Equations with Reflection*, Lecture Notes in Pure and Applied Mathematics (Universitätsverlag Potsdam, 2014).
56. R. Pinnau, C. Totzeck, O. Tse and S. Martin, A consensus-based model for global optimization and its mean-field limit, *Math. Models Methods Appl. Sci.* **27** (2017) 183–204.
57. S. Reich and C. Cotter, *Probabilistic Forecasting and Bayesian Data Assimilation* (Cambridge Univ. Press, 2015).
58. C. Schillings and A. M. Stuart, Analysis of the ensemble Kalman filter for inverse problems, *SIAM J. Numer. Anal.* **55** (2017) 1264–1290.
59. J. Serrin, The problem of Dirichlet for quasilinear elliptic differential equations with many independent variables, *Phil. Trans. R. Soc. London Ser. A* **264** (1969) 413–496.
60. J. Sirignano and K. Spiliopoulos, Mean field analysis of neural networks: A law of large numbers, *SIAM J. Appl. Math.* **80** (2020) 725–752.
61. L. Slominski, Euler’s approximations of solutions of SDEs with reflecting boundary, *Stoch. Proc. Appl.* **94** (2001) 317–337.
62. R. Storn and K. Price, Differential evolution – a simple and efficient heuristic for global optimization over continuous spaces, *J. Global Optim.* **11** (1997) 341–359.
63. A.-S. Sznitman, Nonlinear reflecting diffusion process, and the propagation of chaos and fluctuations associated, *J. Funct. Anal.* **56** (1984) 311–336.
64. A.-S. Sznitman, *Topics in Propagation of Chaos*, École d’Été de Probabilités de Saint-Flour, Vol. 1464 (Springer, 1991), pp. 165–251.
65. H. Tanaka, Stochastic differential equations with reflecting boundary condition in convex regions, *Hiroshima Math. J.* **9** (1979) 163–177.
66. C. Totzeck, Trends in consensus-based optimization, in *Active Particles: Advances in Theory, Models, and Applications*, Vol. 3 (Springer, 2021), pp. 201–226.
67. A. Townsend, Constrained optimization in Chebfun, www.chebfun.org/examples/opt/ConstrainedOptimization.
68. S. Voß, Meta-heuristics: The state of the art, in *Local Search for Planning and Scheduling*, ed. A. Nareyek (Springer, 2001), pp. 1–23.
69. F.-Y. Wang, Distribution dependent reflecting stochastic differential equations, *Sci. China Math.* **66** (2023) 2411–2456.
70. F.-Y. Wang, Exponential ergodicity for singular reflecting McKean–Vlasov SDEs, *Stoch. Proc. Appl.* **160** (2023) 265–293.